Coordinated multi-objective scheduling of a multi-energy virtual power plant considering storages and demand response

Olanlari, Farzin Ghasemi ; Amraee, Turaj ; Moradi Sepahvand, Mojtaba ; Ahmadian, Ali

DOI
10.1049/gtd2.12543

Publication date
2022

Document Version
Final published version

Published in
IET Generation, Transmission and Distribution

Received: 13 April 2022 | Revised: 14 June 2022 | Accepted: 21 June 2022

IET Generation, Transmission & Distribution

DOI: 10.1049/gtd2.12543

The Institution of Engineering and Technology WILEY

ORIGINAL RESEARCH

Coordinated multi-objective scheduling of a multi-energy virtual power plant considering storages and demand response

Farzin Ghasemi Olanlari[1] | **Turaj Amraee**[1] | **Mojtaba Moradi-Sepahvand**[2] | **Ali Ahmadian**[3]

[1]Electrical Engineering Faculty, K.N. Toosi University of Technology, Tehran, Iran

[2]Department of Electrical Sustainable Energy, Delft University of Technology, Delft, The Netherlands

[3]Faculty of Engineering, University of Waterloo, Ontario, Canada

Correspondence
Turaj Amraee, Electrical Engineering Faculty, K.N. Toosi University of Technology, Tehran, Iran.
Email: amraee@kntu.ac.ir

Abstract

A virtual power plant (VPP) is a solution that brings distributed generation (DG) resources together and allows them to be optimally utilized to meet load demands in the presence of technical and pollution constraints. Electricity, heat, and natural gas are interdependent at the levels of generation, transmission, and consumption, and the interactions of these energy sources need to be considered. This paper presents an optimal model for daily operation of a multi-energy virtual power plant (MEVPP), including electric, thermal, and natural gas sectors. MEVPP includes small-scale gas-fired and non-gas-fired DGs, combined heat and power (CHP), power to gas (P2G), boilers, electrical storage, electric vehicles (EV), and thermal storage. Renewable energy resources (RES), including wind turbines (WT), photovoltaic (PV), and PV-thermal (PVT), also supply P2G technology. Smart grid technologies such as price-based demand response (PBDR) and incentive-based demand response (IBDR) are employed for electric loads. The proposed MEVPP model is eligible to participate in day-ahead electricity, natural gas, heat markets, and electrical spinning reserve market. The scheduling model is multi-objective to maximize MEVPP profit and minimize carbon dioxide emissions. The Epsilon constraint method is utilized to solve the problem, and the best Pareto point is chosen using the fuzzy satisfying approach.

1 | INTRODUCTION

1.1 | Background and motivation

Population growth and the introduction of new technologies such as electric vehicles (EVs) are increasing electricity demand, causing an increase in the generation of conventional power plants. This leads to an increase in the production of greenhouse gases such as CO_2. One effective solution to address this concern is to use distributed energy resources (DERs) on the demand side. The use of these resources requires intelligent control technologies to integrate and manage them [1]. A VPP is an aggregation of DER with varying technologies and interruptible and non-interruptible loads controlled by information and communication technologies (ICTs). Additionally, the VPP enables DER to participate in electricity markets by aggregating various resources, enhancing the network's stability and security [2]. Increasing the penetration of gas-fired distributed generations (DGs) such as microturbines (MTs) and fuel cells (FC) increases the natural gas demand. Power to gas (P2G) technology can meet the growing natural gas demand. This technology converts the electricity power of RES to natural gas based on an electrochemical process [3]. Thermal energy, which has a variety of utilizations such as space heating, water warming, drying, distillation, and desalination, is another essential demand of energy that should be met optimally. Photovoltaic-thermal (PVT) is capable of generating electrical and thermal energy from sunlight. Along with providing clean energy and having low operating costs, this unit is highly efficient in comparison to other renewable energy sources (RESs) [4–6]. Utilizing diverse sources of electricity, natural gas, thermal energy generation, and demand response (DR) programs increases the flexibility

of energy supply for these energies' customers while also complicating units' planning, control, and management. The notion of multi-energy virtual power plant (MEVPP) is developed to address this problem.

1.2 | Literature survey

There is notably rich literature regarding the VPPs scheduling, each of which has made breakthroughs on a specific perspective of the problem. In particular, the following studies are considerable.

DERs are not fixed components in a VPP; they vary according to the problem's goal and application. In [7], VPP includes interruptible loads and DR programs that can participate in the day-ahead markets and compete with other conventional power plants. In [8], a VPP includes wind turbines, MTs, energy storage, and DR participating in the day-ahead, real-time, and spinning reserve markets. Reference [9] presents the optimal offering strategy problem for VPP, which includes WT, PV, ESS, and MT. The problem is bi-level that VPP maximizes its profit on the first level, and the frequency market-clearing process is done on the second level. It should be noted that VPP has participated as a price maker in the market. A VPP model for managing and reducing total costs and emissions is presented in [10]. DER in this study include hybrid electric vehicles, wind turbines, PV, MTs, and fuel cells. In [3], a virtual power plant including wind power plant, PV, MT, and P2G units is modelled with DR programs. Research works in [3, 7–10] cover the small diversity of DERs, while resources such as CHP, boiler, HSS and PVT, each with their specific constraints, are not modelled. Considering the large diversity of DERs increases the complexity of the problem.

Unlike micro-grid, the VPP is permanently connected to its upstream network. Thus, through the upstream network, the VPP exchanges energy with wholesale markets such as electricity, natural gas [11], and thermal energy market [12].

Implementing demand response programs requires an energy management system such as a VPP operator. The VPP operator enables DR implementation by applying pricing policies and controlling interruptible loads. VPP can increase its profit by participating in the spinning reserve market with interruptible loads. Another advantage of these programs is the reduction of consumer bills. Generally, DR programs are divided into PBDR and IBDR [13]. Authors in [14] use PBDR programs, including fixed price (FP), time of use (TOU), and real-time pricing (RTP). This study demonstrates that implementing RTP increases retail profits while also smoothing the load profile. According to the article results, [15] used the TOU program to model a micro-grid, which resulted in lower operating costs. According to [16], the FP program smooths the electric demand profile, whereas the IBDR program, in addition to peak shaving, decreases the fluctuations caused by RES. According to [17], the use of IBDR programs increases the participants' profit in both day-ahead and intraday markets while decreasing peak load. In [18], a layered stochastic model is presented using RTP and IBDR demand response programs. In the first layer of this study, RTP prices are determined by an independent system operator (ISO) and are notified to the load aggregator (LA). The LA predicts its loads in the second layer and tries to minimize its costs using demand response programs. Lastly, the loads receive information about demand response programs from LA and maximize their profits according to this information. This study shows that demand response programs have significantly reduced peak load and energy costs.

Regardless of the strengths and weaknesses of the aforementioned works they have considered only electric energy in the modelling and scheduling. However, in the today's modern energy systems, various kinds of energies are integrated together and should be managed simultaneously to reach a global optimum in the energy management procedure. Multi-energy systems integrate a variety of different energy generation sources. These systems provide numerous benefits, including cost savings, reduced emissions, increased system reliability and flexibility, and improved system performance and efficiency [19]. In [20], an active distribution network is used to supply electric, heating, and cooling demands. This study shows that with multi-energy sources, operating costs and local marginal prices have decreased. The paper [21] presents a new approach to planning a multi-energy micro-grid. In this research, combined cooling, heating, and power (CCHP), P2G units, storage facilities, and wind turbines have been used to participate in electricity and natural gas markets; the results show a reduction in risk and operating costs. A VPP is modelled by considering the network security constraints in [4]; the results show that the use of multi-energy sources increases the profit of the VPP. Additionally, the usage of PVT reduces the VPP's dependency on CHP and boilers to meet thermal load requirements. In [22], the planning of hybrid energy storage including compressed air energy storage (CAES), P2G, and thermal energy storage has been done. The article results show that if all three types of storage are used, the overall profit of this unit will increase. In [23], an energy hub system is presented to reduce costs and increase energy efficiency. This system includes WT, P2G, CAES and shiftable loads. This study shows that considering the interactions between electrical energy and natural gas reduces operation costs.

1.3 | Research gaps

Most of previous research works consider a ingle objective function for VPP, while the problem can be optimized from different perspectives using multi-objective optimization methods such as Pareto-based methods [24], weighting method [25], and methods of converting several objective functions into one objective function [26]. In addition, any parameter that is related to the future has uncertainty and must be managed using a proper uncertainty modelling approach such as robust optimization [27], scenario generation [28], and artificial neural networks [29]. Wind speed, solar radiation, load demands, and market prices are the parameters with significant uncertainty [2].

TABLE 1 Comparison of reviewed articles based on the components, emission and multi energy consideration

	Components												
Ref.	WT	PV	PVT	MT	FC	CHP	Boiler	EV	ESS	HSS	P2G	Emission	Multi energy
[3]	✓	✓		✓							✓	✓	✓
[4]	✓	✓	✓	✓		✓	✓		✓				✓
[7]				✓									✓
[8]	✓			✓					✓				
[10]	✓	✓		✓	✓			✓				✓	
[21]	✓			✓		✓	✓		✓			✓	✓
[24]	✓	✓		✓		✓	✓		✓			✓	✓
[25]	✓	✓		✓				✓			✓	✓	✓
[26]	✓	✓		✓	✓				✓			✓	
[27]	✓					✓	✓	✓	✓	✓	✓		✓
[28]	✓	✓		✓		✓	✓	✓	✓	✓			✓
[29]	✓			✓		✓		✓	✓			✓	✓
This paper	✓	✓	✓	✓	✓	✓	✓	✓	✓	✓	✓	✓	✓

TABLE 2 Comparison of reviewed articles based on market participation, DR programs, type of formulation, objective function, type of optimization and solution method

	Market			DR		Formulation type				Solution method	
Ref.	Electricity	Natural gas	Thermal	IBDR	PBDR	Deterministic	Stochastic	Objective function	Optimization type	Mathematical	Heuristic
[3]	✓			✓	✓		✓	Max profit	MIP	✓	
[4]	✓						✓	Max profit	MIP	✓	
[7]	✓			✓	✓	✓		Bi-level	MIP	✓	
[8]	✓			✓			✓	Max profit	MIP	✓	
[10]						✓		Min costs	MIP	✓	
[21]	✓	✓					✓	Min costs	MIP	✓	
[24]	✓						✓	Multi-objective	MINLP		✓
[25]				✓	✓		✓	Multi-objective	MIP	✓	
[26]	✓					✓		Multi-objective	MINLP		✓
[27]	✓	✓	✓	✓			✓	Min costs	MIP	✓	
[28]	✓			✓			✓	Max profit	MIP	✓	
[29]	✓						✓	Max profit	MIP	✓	
This paper	✓	✓	✓	✓	✓		✓	Multi-objective	MIP	✓	

Regarding these issues, the lack of a comprehensive operating model for an MEVPP and its interactions is a critical research gap in previous works. The coupling between electricity, gas and heat in generation, consumption and storage sides impact the energy scheduling significantly. Such an important issue has not been well investigated in previous works. Tables 1 and 2 represent the classification of numerous types of research reviewed in the literature review section based on factors such as the kind of DER, participation in different markets, consideration of emission produced, DR programs, formulation, and type of problem. Tables 1 and 2 are provided to compare the articles better. As can be seen in these tables, the units utilized in references [4, 23, 24] have a good variation; however, the impact of pollution is not considered in these articles. In contrast, reference [26] considers the impact of pollution, but no unit in this article produces or consumes natural gas. References [21, 24] have used multi-objective optimization in their model. However, their problem is modelled as mixed integer non-linear programming (MINLP), which increases the problem-solving time and might get stuck in the local optimum solution. Finally,

in reference [22], multi-objective optimization is used as an MILP problem, but the virtual power plant participation in energy markets is not considered. This paper includes features such as a wide range of electrical, thermal, and natural gas units, participation in day-ahead energy markets and the spinning reserve market, multi-objective optimization, and mixed integer linear programming (MILP) modelling.

1.4 | Novelties and contributions

In this paper, generation, consumption, and storage in the electrical, thermal, and natural gas sectors are simultaneously scheduled using a comprehensive MEVPP considering the related technical constraints and interactions. In addition to the diversity of generation resources, the two essential goals including maximizing the MEVPP's profit and minimizing the emission amount are considered. The proposed mathematic problem is formulated as a multi-objective problem. The main contributions of this work can be summarized as follows:

- As the couplings and interactions between different energy careers impact the energy scheduling and efficiency significantly, a comprehensive mathematical model is proposed for MEVPP scheduling that includes generation, consumption and storage of electricity, natural gas, and thermal energies regarding technical constraints and interactions. P2G option is included to produce natural gas, PVT is utilized to generate electrical and thermal energy from sunlight, and EVs are taken into account to increase system flexibility.
- Behind the meter solutions including the PBDR and IBDR programs are modelled to smooth the load profile and increase the profit of MEVPP.
- A multi-objective optimization is proposed to maximize the profit of the MEVPP and minimize the emission using the Epsilon constraint method and the fuzzy satisfying approach to select the best Pareto solution.
- The proposed MEVPP is participated in the day-ahead markets for the exchange of electricity, natural gas, and thermal energy, and the spinning reserve market of electricity. The scenario generation and reduction method is used to handle uncertainty parameters, including wind speed, solar radiation, electricity demand, day-ahead electricity market price, and EVs' behaviour.

1.5 | Paper structure

The paper is organized as follows. In Section 2, the proposed MEVPP framework and mathematical formulation are described. Uncertainty modelling and multi-objective optimization are presented in Section 3. In Section 4, the simulation results are presented, and finally, in the Section 5, the conclusion is stated.

2 | THE MEVPP FRAMEWORK AND MATHEMATICAL FORMULATION

The proposed framework developed by merging multiple electricity, heat, and natural gas generation units builds an MEVPP that can provide varied electrical, thermal, and gas demands of the network. Figure 1 illustrates the structure of the studied MEVPP, which includes renewable units, energy storage, micro-turbines, gas-fired and non-gas-fired DGs, boilers, P2G, and electric vehicles. Some units, such as CHP and PVT, can simultaneously generate two electrical and thermal energy types. It should be noted that renewable power plants supply the input power of P2G technology. This allows P2G to produce natural gas using clean electricity, and also, power fluctuations of renewable power plants do not affect the power system. As shown in Figure 1, the penetration of DER in the understudy electrical network is high, and these resources can easily meet the electricity demand. As a result, there is no need to use renewable power plants to meet the electricity demand in this network. The modelled framework can interchange all types of energy with the upstream network and participate in the day-ahead electricity, heat, and natural gas markets as price-takers. The ability to participate in the electricity spinning reserve market is also considered. It should be mentioned that PBDR and IBDR programs have also been applied to electrical loads.

The utilized MEVPP's energy-generating components are classified into three types: electricity, natural gas, and thermal energy generators. Micro-turbines, fuel cells, CHP, batteries, and electric vehicles are examples of power generation units. The P2G unit generates natural gas, while renewable power plants such as WT, PV, and PVT supply the electricity required by the P2G unit. Finally, thermal energy is generated by PVT, boiler, CHP, and heat storage system (HSS). The following is the formulation of the MEVPP components and the problem's objective functions.

2.1 | RES modelling

This paper examines WT, PV, and PVT power plants that generate energy by employing wind speed, sunlight, and ambient temperature. The PVT power plant can generate both electrical and thermal energy simultaneously. Furthermore, because renewable power plants do not utilize any fuel, their operation costs are negligible. The detail and formulation of mentioned renewable power plants are derived from [4].

2.2 | DG modelling

DGs include gas-fired and non-gas-fired generators. In this paper, the fuel cell is considered as gas-fired DG. These units generate electricity for the electrical network and, at the same time, are an industrial consumer for the natural gas network [29–31]. The operating cost of the DGs is given in Equation (1)

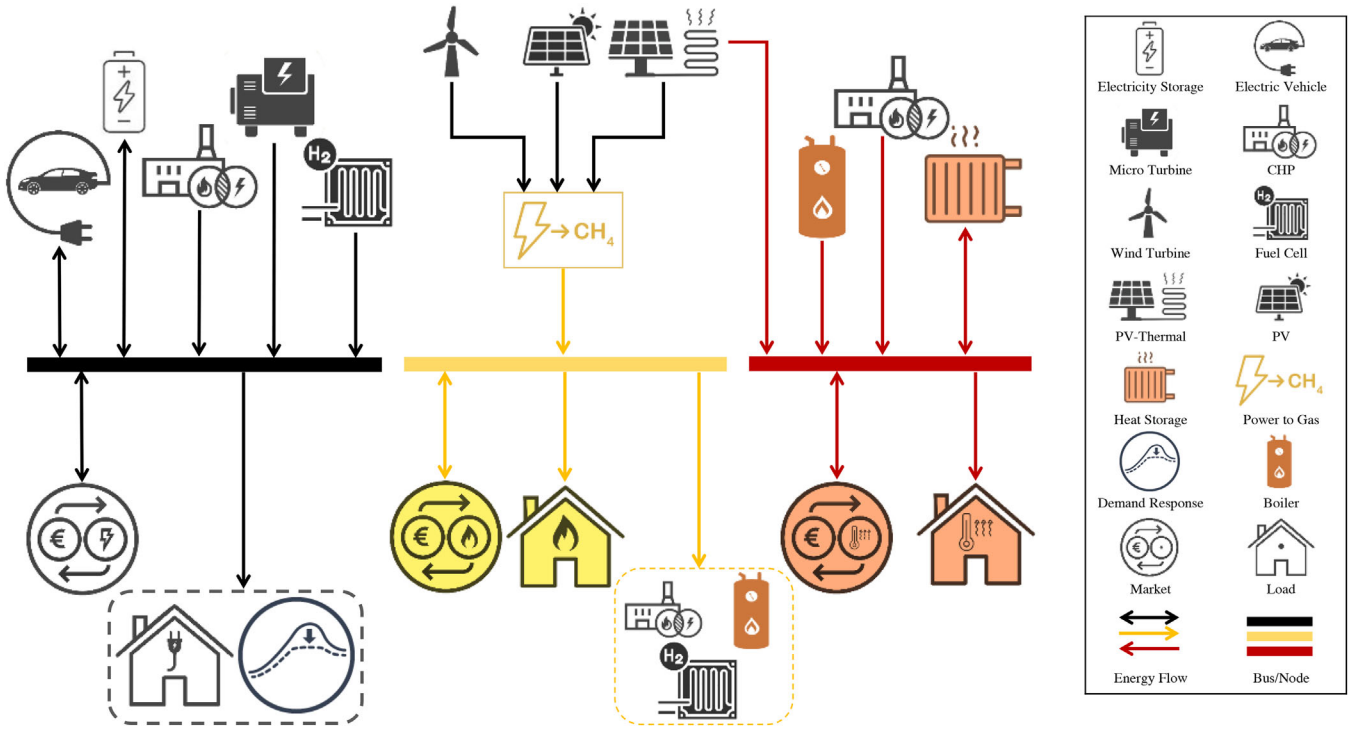

FIGURE 1 Multi energy virtual power plant framework

as the sum of the production, startup, and shutdown costs, which are defined in Equations (2)–(4), respectively. Equation (5) calculates the amount of fuel consumed by DG3, and Equation (6) calculates the emission produced by these units. Each unit's spinning reserve, minimum, and maximum generation limits are given in Equations (7) and (8), respectively. Other DG constraints include the ramp rate and the minimum on and off time, computed in Equations (9)–(12). Constraints (13) and (14) count the number of hours each DG is on and off. The method in [31] has been used to linearize the constraints of (3), (4), and (11)–(14).

$$C_{dg,t,s} = C^{prod}_{dg,t,s} + C^{SU}_{dg,t} + C^{SD}_{dg,t} \quad \forall dg \epsilon \Omega_{DG}, t \epsilon \Omega_T, s \epsilon \Omega_S \tag{1}$$

$$C^{prod}_{dg,t,s} = a_{dg} \times \left(P_{dg,t,s} + Res_{dg,t,s}\right) + b_{dg} \times u_{dg,t} \quad \forall dg \epsilon \Omega_{DG}, t \epsilon \Omega_T, s \epsilon \Omega_S \tag{2}$$

$$C^{SU}_{dg,t} = SUC_{dg} \times u_{dg,t} \times \left(1 - u_{dg,t-1}\right) \quad \forall dg \epsilon \Omega_{DG}, t \epsilon \Omega_T \tag{3}$$

$$C^{SD}_{dg,t} = SDC_{dg} \times u_{dg,t-1} \times \left(1 - u_{dg,t}\right) \quad \forall dg \epsilon \Omega_{DG}, t \epsilon \Omega_T \tag{4}$$

$$F_{dg,t,s} = HV^{NG} \times \frac{P_{dg,t,s} + Res_{dg,t,s}}{\eta_{dg}} \quad \forall dg \# 3 \epsilon \Omega_{DG}, t \epsilon \Omega_T, s \epsilon \Omega_S \tag{5}$$

$$E_{dg,t,s} = P_{dg,t,s} \times \mu^{CO_2}_{dg} \quad \forall dg \epsilon \Omega_{DG}, t \epsilon \Omega_T, s \epsilon \Omega_S \tag{6}$$

$$Res_{dg,t,s} \le P^{max}_{dg} \times u_{dg,t} - P_{dg,t,s} \quad \forall dg \epsilon \Omega_{DG}, t \epsilon \Omega_T, s \epsilon \Omega_S \tag{7}$$

$$P^{min}_{dg} \times u_{dg,t} \le P_{dg,t,s} + Res_{dg,t,s} \le P^{max}_{dg} \times u_{dg,t} \quad \forall dg \epsilon \Omega_{DG}, t \epsilon \Omega_T, s \epsilon \Omega_S \tag{8}$$

$$\left(P_{dg,t,s} - P_{dg,t-1,s}\right) + Res_{dg,t,s} \le RU_{dg} \quad \forall dg \epsilon \Omega_{DG}, t \epsilon \Omega_T, s \epsilon \Omega_S \tag{9}$$

$$P_{dg,t-1,s} - P_{dg,t,s} \le RD_{dg} \quad \forall dg \epsilon \Omega_{DG}, t \epsilon \Omega_T, s \epsilon \Omega_S \tag{10}$$

$$\left(X^{on}_{dg,t-1} - UT^{on}_{dg}\right) \times \left(u_{dg,t-1} - u_{dg,t}\right) \ge 0 \quad \forall dg \epsilon \Omega_{DG}, t \epsilon \Omega_T \tag{11}$$

$$X^{on}_{dg,t} = \left(1 - u_{dg,t-1}\right) \times u_{dg,t} + u_{dg,t} \times u_{dg,t-1} \times \left(1 + X^{on}_{dg,t-1}\right) \quad \forall dg \epsilon \Omega_{DG}, t \epsilon \Omega_T \tag{12}$$

$$\left(X^{off}_{dg,t-1} - DT^{off}_{dg}\right) \times \left(u_{dg,t} - u_{dg,t-1}\right) \ge 0 \quad \forall dg \epsilon \Omega_{DG}, t \epsilon \Omega_T \tag{13}$$

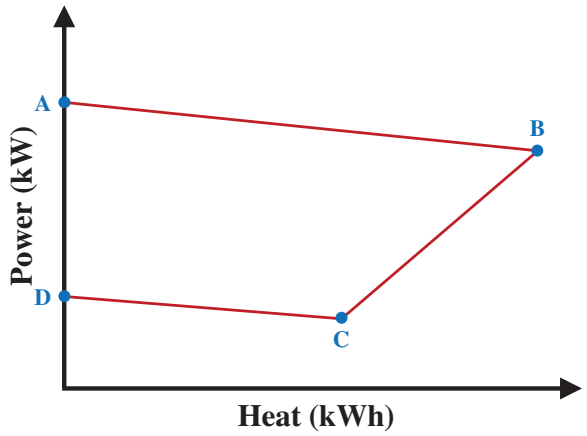

FIGURE 2 Operation range of CHP unit

$$X_{dg,t}^{off} = \left(1 - u_{dg,t}\right)\ u_{dg,t-1} + \left(1 - u_{dg,t}\right)\left(1 - u_{dg,t-1}\right) \times \left(1 + X_{dg,t-1}^{on}\right) \quad \forall dg \epsilon \Omega_{DG}, t \epsilon \Omega_T \tag{14}$$

2.3 | CHP modelling

The CHP unit is responsible for the simultaneous generation of electrical and thermal energy, and at the same time, it is an industrial consumer for the natural gas network. This unit's operational range is a quadrilateral, as seen in Figure 2. The maximum and minimum electrical power of this unit are represented by points A and C, respectively. Similarly, points B and D represent the maximum and minimum heat output of this unit, respectively [4, 24]. The operation cost of the CHP, including the production cost, startup, and shutdown costs, is given in Equations (15)–(17). Also, the amount of fuel consumed and the emission produced are calculated in Equations (18) and (19), respectively. Constraints (20) and (21) determine this unit's minimum and maximum thermal and electrical power, respectively. Equations (22)–(24) define the operational range of the CHP, as shown in Figure 2. The ramp up, ramp down, and the spinning reserve capacity of CHP are calculated in Equations (25)–(27), respectively.

$$C_{chp,t,s} = F_{chp,t,s} \times \pi_t^{NG} + C_{chp,t}^{SU} + C_{chp,t}^{SD} \quad \forall chp \epsilon \Omega_{CHP},\ t \epsilon \Omega_T,\ s \epsilon \Omega_S \tag{15}$$

$$C_{chp,t}^{SU} = SUC_{chp} \times u_{chp,t} \times \left(1 - u_{chp,t-1}\right) \quad \forall chp \epsilon \Omega_{CHP},\ t \epsilon \Omega_T \tag{16}$$

$$C_{chp,t}^{SD} = SDC_{chp} \times u_{chp,t-1} \times \left(1 - u_{chp,t}\right) \quad \forall chp \epsilon \Omega_{CHP},\ t \epsilon \Omega_T \tag{17}$$

$$F_{chp,t,s} = HV^{NG} \times \frac{P_{chp,t,s} + Res_{chp,t,s}}{\eta_{chp}} \quad \forall chp \epsilon \Omega_{CHP},\ t \epsilon \Omega_T,\ s \epsilon \Omega_S \tag{18}$$

$$E_{chp,t,s} = P_{chp,t,s} \times \mu_{chp}^{CO_2} \quad \forall chp \epsilon \Omega_{CHP},\ t \epsilon \Omega_T,\ s \epsilon \Omega_S \tag{19}$$

$$H_{chp}^{A} \times u_{chp,t} \le H_{chp,t,s} \le H_{chp}^{B} \times u_{chp,t} \quad \forall chp \epsilon \Omega_{CHP},\ t \epsilon \Omega_T,\ s \epsilon \Omega_S \tag{20}$$

$$P_{chp}^{C} \times u_{chp,t} \le P_{chp,t,s} + Res_{chp,t,s} \le P_{chp}^{A} \times u_{chp,t} \quad \forall chp \epsilon \Omega_{CHP},\ t \epsilon \Omega_T,\ s \epsilon \Omega_S \tag{21}$$

$$\left(P_{chp,t,s} + Res_{chp,t,s}\right) - P_{chp}^{A} - \frac{P_{chp}^{A} - P_{chp}^{B}}{H_{chp}^{A} - H_{chp}^{B}} \times \left(H_{chp,t,s} - H_{chp}^{A}\right) \le 0 \quad \forall chp \epsilon \Omega_{CHP},\ t \epsilon \Omega_T,\ s \epsilon \Omega_S \tag{22}$$

$$\left(P_{chp,t,s} + Res_{chp,t,s}\right) - P_{chp}^{B} - \frac{P_{chp}^{B} - P_{chp}^{C}}{H_{chp}^{B} - H_{chp}^{C}} \times \left(H_{chp,t,s} - H_{chp}^{B}\right) \ge -M \times \left(1 - u_{chp,t}\right) \quad \forall chp \epsilon \Omega_{CHP},\ t \epsilon \Omega_T,\ s \epsilon \Omega_S \tag{23}$$

$$\left(P_{chp,t,s} + Res_{chp,t,s}\right) - P_{chp}^{C} - \frac{P_{chp}^{C} - P_{chp}^{D}}{H_{chp}^{C} - H_{chp}^{D}} \times \left(H_{chp,t,s} - H_{chp}^{C}\right) \ge -M \times \left(1 - u_{chp,t}\right) \quad \forall chp \epsilon \Omega_{CHP},\ t \epsilon \Omega_T,\ s \epsilon \Omega_S \tag{24}$$

$$\left(P_{chp,t,s} - P_{chp,t-1,s}\right) + Res_{chp,t,s} \le RU_{chp} \quad \forall chp \epsilon \Omega_{CHP},\ t \epsilon \Omega_T,\ s \epsilon \Omega_S \tag{25}$$

$$P_{chp,t-1,s} - P_{chp,t,s} \le RD_{chp} \quad \forall chp \epsilon \Omega_{CHP},\ t \epsilon \Omega_T,\ s \epsilon \Omega_S \tag{26}$$

$$Res_{chp,t,s} \le P_{chp}^{A} \times u_{chp,t} - P_{chp,t,s} \quad \forall chp \epsilon \Omega_{CHP},\ t \epsilon \Omega_T,\ s \epsilon \Omega_S \tag{27}$$

2.4 | ESS modelling

An electricity storage system is charged when there is excessive generation and discharged during high electrical load. The degradation cost of ESS is considered in Equation (28) [29]. This unit's minimum and maximum charge and discharge rates are given in Equations (29) and (30). Equation (31) is provided to prevent charging and discharging simultaneously. State of Charge (SOC), the minimum and maximum SOC of this unit are calculated in Equations (32) and (33), respectively. Constraint

(34) indicates that the SOC at the end of the day should be equal to the SOC at the beginning of the next day.

$$C_{ess,t,s} = a_{ess} \times \left(P^{ch}_{ess,t,s} + P^{dch}_{ess,t,s}\right) + b_{ess} \times \left(u^{ch}_{ess,t} + u^{dch}_{ess,t}\right) \quad \forall ess \epsilon \Omega_{ESS},\ t \epsilon \Omega_T,\ s \epsilon \Omega_S \tag{28}$$

$$P^{ch,min}_{ess} \times u^{ch}_{ess,t} \le P^{ch}_{ess,t,s} \le P^{ch,max}_{ess} \times u^{ch}_{ess,t} \quad \forall ess \epsilon \Omega_{ESS},\ t \epsilon \Omega_T,\ s \epsilon \Omega_S \tag{29}$$

$$P^{dch,min}_{ess} \times u^{dch}_{ess,t} \le P^{dch}_{ess,t,s} \le P^{dch,max}_{ess} \times u^{dch}_{ess,t} \quad \forall ess \epsilon \Omega_{ESS},\ t \epsilon \Omega_T,\ s \epsilon \Omega_S \tag{30}$$

$$u^{ch}_{ess,t} + u^{dch}_{ess,t} \le 1 \quad \forall ess \epsilon \Omega_{ESS},\ t \epsilon \Omega_T \tag{31}$$

$$SOC_{ess,t,s} = SOC_{ess,t-1,s} + P^{ch}_{ess,t,s} \times \eta^{ch}_{ess} - \frac{P^{dch}_{ess,t,s}}{\eta^{dch}_{ess}} \quad \forall ess \epsilon \Omega_{ESS},\ t \epsilon \Omega_T,\ s \epsilon \Omega_S \tag{32}$$

$$SOC^{min}_{ess} \le SOC_{ess,t,s} \le SOC^{max}_{ess} \quad \forall ess \epsilon \Omega_{ESS},\ t \epsilon \Omega_T,\ s \epsilon \Omega_S \tag{33}$$

$$SOC_{ess,t24,s} = SOC_{ess,t0} \quad \forall ess \epsilon \Omega_{ESS},\ s \epsilon \Omega_S \tag{34}$$

2.5 | EV modelling

EVs are new technologies that are also known as mobile storage. The battery of these vehicles is rechargeable, so the MEVPP operator can use them to increase network flexibility [32]. Equation (35) shows the cost of charging and discharging EVs. Equations (36) and (37) show the maximum charging and discharge rate of each EV, which is carried out in the parking lot. Equation (38) shows that an EV's SOC changes in a parking lot and while traveling. Also, the maximum and minimum SOC limits are specified in Equation (39). It should be noted that the battery charge rate, battery capacity, and energy consumption of each EV are determined by the vehicle model. Equation (40) calculates the amount of energy consumed by an EV during travel in miles.

$$C_{EV,t,s} = P^{dch}_{EV,t,s} \times C^{dch,EV} - P^{ch}_{EV,t,s} \times C^{ch,EV} \quad \forall ev \epsilon \Omega_{EV},\ t \in t^{Parking},\ s \epsilon \Omega_S \tag{35}$$

$$0 \le P^{ch}_{EV,t,s} \le CR_{EV} \times u^{ch}_{EV,t} \quad \forall ev \epsilon \Omega_{EV},\ t \in t^{Parking},\ s \epsilon \Omega_S \tag{36}$$

$$0 \le P^{dch}_{EV,t,s} \le CR_{EV} \times u^{dch}_{EV,t} \quad \forall ev \epsilon \Omega_{EV},\ t \in t^{Parking},\ s \epsilon \Omega_S \tag{37}$$

$$SOC_{EV,t,s} = SOC_{EV,t-1,s} + P^{ch}_{EV,t,s} \times \eta^{ch}_{EV} - \frac{P^{dch}_{EV,t,s}}{\eta^{dch}_{EV}} - EC^{Trip}_{EV,t} \quad \forall ev \epsilon \Omega_{EV},\ t \epsilon \Omega_T,\ s \epsilon \Omega_S \tag{38}$$

$$SOC^{min}_{EV} \le SOC_{EV,t,s} \le SOC^{max}_{EV} \quad \forall ev \epsilon \Omega_{EV},\ t \epsilon \Omega_T,\ s \epsilon \Omega_S \tag{39}$$

$$EC^{Trip}_{EV,t} = Mileage_{EV,t} \times ECPM_{EV} \quad \forall ev \epsilon \Omega_{EV},\ t \in t^{Trip} \tag{40}$$

2.6 | DR modelling

PBDR programs encourage electricity consumers to shift their consumption by implementing proper pricing. This reduces the peak and smooths the load profile [33]. One of the PBDR programs used in this paper is RTP. In this method, the price of electricity is different during the day. As a result, consumption increases during off-peak hours and decreases during peak hours. Equation (41) limits the minimum and maximum amount of electric load shifting each hour. It should be noted that the total load changes during the day should be equal to zero (Equation (42)).

$$-PD^{initial}_{t,s} \times pr^{PBDR} \le \Delta L^{PBDR}_{t,s} \le PD^{initial}_{t,s} \times pr^{PBDR} \forall t \epsilon \Omega_T,\ s \epsilon \Omega_S \tag{41}$$

$$\sum_{t \epsilon \Omega_T} \Delta L^{PBDR}_{t,s} = 0 \forall s \epsilon \Omega_S \tag{42}$$

In IBDR programs, the MEVPP operator signs a contract with interruptible loads to reduce loads in emergency conditions. The MEVPP operator also pays participants of these programs to reduce their loads. The MEVPP operator can also use the capacity of interruptible loads in the spinning reserve market to increase its profit [34]. It should be noted that the curve of interruptible loads consists of three load blocks that are arranged in ascending order. Equation (43) shows the cost that the MEVPP must pay for interruptible loads. Equation (44) shows the amount of load reduced in each block, and Equation (45) calculates the maximum amount of load that can be reduced in each block. Equations (46) and (47) determine the price of each load block. Equation (48) also shows the capacity of interruptible loads considered to participate in the spinning

reserve market.

$$C_{t,s}^{IBDR} = \sum_{b\epsilon\Omega_B} \pi_{t,b}^{IBDR} \times \Delta L_{t,b,s}^{IBDR} \quad \forall t\epsilon\Omega_T,\ s\epsilon\Omega_S \tag{43}$$

$$\Delta L_{t,b,s}^{IBDR} \le L_{t,b,s}^{IBDR} - L_{t,b-1,s}^{IBDR} \quad \forall t\epsilon\Omega_T,\ s\epsilon\Omega_S,\ b\epsilon\Omega_B \tag{44}$$

$$L_{t,b,s}^{IBDR} = PD_{t,s}^{initial} \times pr^{IBDR} \times \frac{b}{N^B} \quad \forall t\epsilon\Omega_T,\ s\epsilon\Omega_S,\ b\epsilon\Omega_B \tag{45}$$

$$\pi_{t,b}^{IBDR} = (1 + 0.2 \times b) \times \pi^{IBDR,base} \quad \forall t\epsilon\Omega_T,\ b\epsilon\Omega_B \tag{46}$$

$$\pi_{t,b}^{IBDR} = \pi^{IBDR,base} \quad \forall t\epsilon\Omega_T,\ b = 1 \tag{47}$$

$$Res_{t,s}^{IBDR} \le PD_{t,s}^{initial} \times pr^{IBDR} - \sum_{b\epsilon\Omega_B} \Delta L_{t,b,s}^{IBDR} \quad \forall t\epsilon\Omega_T,\ s\epsilon\Omega_S \tag{48}$$

2.7 | Boiler modelling

The boiler is one of the main components of the thermal network that generates heat by burning natural gas [27]. Equation (49) shows the operating cost of this unit, which is a function of its fuel consumption. In Equation (50), the boiler's fuel consumption is calculated using the heat value of natural gas and the boiler's efficiency. The amount of CO_2 produced by the boiler per kW is shown in Equation (51). This unit's maximum and minimum thermal power are also determined by Equation (52).

$$C_{boiler,t,s} = F_{boiler,t,s} \times \pi_t^{NG} \quad \forall boiler\epsilon\Omega_{Boiler},\ t\epsilon\Omega_T,\ s\epsilon\Omega_S \tag{49}$$

$$F_{boiler,t,s} = HV^{NG} \times \frac{H_{boiler,t,s}}{\eta_{boiler}} \quad \forall boiler\epsilon\Omega_{Boiler}, t\epsilon\Omega_T,\ s\epsilon\Omega_S \tag{50}$$

$$E_{boiler,t,s} = H_{boiler,t,s} \times \mu_{boiler}^{CO_2} \quad \forall boiler\epsilon\Omega_{Boiler}, t\epsilon\Omega_T,\ s\epsilon\Omega_S \tag{51}$$

$$H_{boiler,t}^{min} \times u_{boiler,t} \le H_{boiler,t,s} \le H_{boiler,t}^{max} \times u_{boiler,t} \quad \forall boiler\epsilon\Omega_{Boiler}, t\epsilon\Omega_T,\ s\epsilon\Omega_S \tag{52}$$

2.8 | HSS modelling

HSS is responsible for storing thermal energy. This unit stores excess heat energy and releases it when needed. HSS can also increase MEVPP profits in the thermal energy market. As a result, as the market price rises, it discharges energy. The degradation cost, minimum and maximum output thermal power, and SOC are all the same as the ESS unit, except that thermal power is substituted instead of electrical power.

2.9 | P2G modelling

According to Figure 3, P2G technology consists of electrolyser, methanation process, and natural gas storage [21]. In an electrolyser, water is transformed to hydrogen using electrical energy provided by RES. Then, in the methanation process, methane gas is produced by combining hydrogen gas and carbon dioxide. The methane produced is stored in a natural gas storage tank or injected directly into the grid. P2G reduces the impact of RES uncertainties on the network. Carbon dioxide gas in this technology is collected by the carbon capture process, which reduces air pollution. The cost of this unit includes the operation cost, maintenance cost of RES, and the cost of carbon dioxide absorption, all of which are assumed to be covered by a government subsidy. Equation (53) calculates the amount of natural gas generated by the input electrical energy. The minimum and maximum capacities of P2G are determined according to Equation (54). RES supplies the P2G input power according to Equation (55). The minimum and maximum charge and discharge rates of natural gas in the storage of this unit are specified in Equations (56) and (57). Equation (58) prevents simultaneous charging and discharging at each hour. Equations (59)–(61) show the SOC of natural gas storage. Equation (62) shows the amount of output natural gas in P2G.

$$G_{P2G,t,s}^{ch} + G_{P2G,t,s}^{CH_4} = HV^{NG} \times P_{P2G,t,s} \times \eta_{P2G} \quad \forall p2g\epsilon\Omega_{P2G}, t\epsilon\Omega_T,\ s\epsilon\Omega_S \tag{53}$$

$$P_{P2G}^{min} \le P_{P2G,t,s} \le P_{P2G}^{max} \quad \forall p2g\epsilon\Omega_{P2G}, t\epsilon\Omega_T,\ s\epsilon\Omega_S \tag{54}$$

$$P_{P2G,t,s} \le \sum_{pv\epsilon\Omega_{PV}} P_{PV,t,s} + \sum_{pvt\epsilon\Omega_{PVT}} P_{PVT,t,s} + \sum_{wt\epsilon\Omega_{WT}} P_{WT,t,s} \quad \forall p2g\epsilon\Omega_{P2G}, t\epsilon\Omega_T,\ s\epsilon\Omega_S \tag{55}$$

$$G_{P2G}^{ch,min} \times u_{P2G,t}^{ch} \le G_{P2G,t,s}^{ch} \le G_{P2G}^{ch,max} \times u_{P2G,t}^{ch} \quad \forall p2g\epsilon\Omega_{P2G}, t\epsilon\Omega_T,\ s\epsilon\Omega_S \tag{56}$$

$$G_{P2G}^{dch,min} \times u_{P2G,t}^{dch} \le G_{P2G,t,s}^{dch} \le G_{P2G}^{dch,max} \times u_{P2G,t}^{dch} \quad \forall p2g\epsilon\Omega_{P2G}, t\epsilon\Omega_T,\ s\epsilon\Omega_S \tag{57}$$

$$u_{P2G,t}^{ch} + u_{P2G,t}^{dch} \le 1 \quad \forall p2g\epsilon\Omega_{P2G}, t\epsilon\Omega_T \tag{58}$$

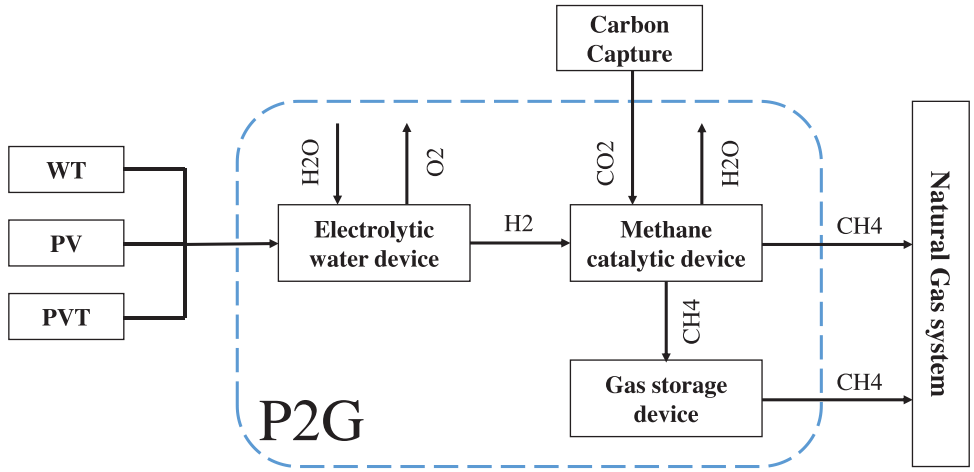

FIGURE 3 Schematic of P2G facility

$$GS_{P2G,t,s} = GS_{P2G,t-1,s} + G^{ch}_{P2G,t,s} \times \eta^{ch}_{P2G} - \frac{G^{dch}_{P2G,t,s}}{\eta^{dch}_{P2G}} \quad \forall p2g \epsilon \Omega_{P2G}, t \epsilon \Omega_T, \ s \epsilon \Omega_S \quad (59)$$

$$GS^{min}_{P2G} \le GS_{P2G,t,s} \le GS^{max}_{P2G} \quad \forall p2g \epsilon \Omega_{P2G}, t \epsilon \Omega_T, \ s \epsilon \Omega_S \quad (60)$$

$$GS_{P2G,t24,s} = GS_{P2G,t0} \quad \forall p2g \epsilon \Omega_{P2G}, s \epsilon \Omega_S \quad (61)$$

$$G_{P2G,t,s} = G^{CH_4}_{P2G,t,s} + G^{dch}_{P2G,t,s} \quad \forall p2g \epsilon \Omega_{P2G}, t \epsilon \Omega_T, \ s \epsilon \Omega_S \quad (62)$$

The amount of carbon dioxide absorbed by P2G is modelled as Equations (63)–(66). The (63) specifies the amount of carbon dioxide required by the P2G unit. The amount of carbon dioxide cannot be more than the total amount of emission produced by the units of the MEVPP, which is given in Equation (64). Equation (65) shows the total amount of emission absorbed through the carbon capture process, and Equation (66) specifies the amount of power required in the carbon capture process.

$$E_{P2G,t,s} = \mu^{CO_2}_{P2G} \times P_{P2G,t,s} \quad \forall p2g \epsilon \Omega_{P2G}, t \epsilon \Omega_T, \ s \epsilon \Omega_S \quad (63)$$

$$E_{P2G,t,s} \le E^{Total}_{t,s} \quad \forall p2g \epsilon \Omega_{P2G}, t \epsilon \Omega_T, \ s \epsilon \Omega_S \quad (64)$$

$$E^{Total}_{t,s} = \eta^{CC} \times \left(\sum_{dg \epsilon \Omega_{DG}} E_{dg,t,s} + \sum_{chp \epsilon \Omega_{CHP}} E_{chp,t,s} + \sum_{boiler \epsilon \Omega_{Boiler}} E_{boiler,t,s} \right) \times \forall t \epsilon \Omega_T, \ s \epsilon \Omega_S \quad (65)$$

$$P^{CC}_{t,s} = \rho^{CC} \times E^{Total}_{t,s} \quad \forall t \epsilon \Omega_T, \ s \epsilon \Omega_S \quad (66)$$

2.10 | Objective functions

The objective functions of the problem include maximizing the profit of the MEVPP and minimizing the amount of emission production, which are given in Equations (67) and (78). The first objective function includes profits from energy exchange with different markets, profits from the sale of energy to consumers, and unit costs [27]. Profits from energy markets, including the day-ahead markets for electricity, heat, and natural gas, and the electricity spinning reserve market are specified in Equations (68)–(72). It should be noted that MEVPP participates in the energy markets as a price-taker. Profits from the sale of energy to consumers included electrical, thermal and natural gas are also given in Equations (73)–(76). Equation (77) calculates the total cost of MEVPP units. These costs included the DG, CHP, and boiler operation costs and the degradation costs of ESS, EV, and HSS that were calculated in previous sections.

$$f_1 = \max \sum_{s \epsilon \Omega_S} Prob_s \sum_{t \epsilon \Omega_T} \left(Profit^{market}_{t,s} + Profit^{retail}_{t,s} - Cost^{Units}_{t,s} \right) \quad (67)$$

$$Profit^{market}_{t,s} = \left(R^{power,DA}_{t,s} + R^{power,res}_{t,s} \right) + R^{NG,DA}_{t,s} + R^{Heat,DA}_{t,s} \quad \forall t \epsilon \Omega_T, \ s \epsilon \Omega_S \quad (68)$$

$$R^{power,DA}_{t,s} = \pi^{power}_{t} \times P^{DA}_{t,s} \quad \forall t \epsilon \Omega_T, \ s \epsilon \Omega_S \quad (69)$$

$$R^{power,res}_{t,s} = \pi^{res}_{t} \times P^{res}_{t,s} \quad \forall t \epsilon \Omega_T, \ s \epsilon \Omega_S \quad (70)$$

$$R_{t,s}^{NG,DA} = \pi_t^{NG} \times G_{t,s}^{DA} \quad \forall t \epsilon \Omega_T,\ s \epsilon \Omega_S \tag{71}$$

$$R_{t,s}^{Heat,DA} = \pi_t^{Heat} \times H_{t,s}^{DA} \quad \forall t \epsilon \Omega_T,\ s \epsilon \Omega_S \tag{72}$$

$$Profit_{t,s}^{retail} = R_{t,s}^{retail,power} + R_{t,s}^{retail,NG} + R_{t,s}^{retail,Heat} \quad \forall t \epsilon \Omega_T,\ s \epsilon \Omega_S \tag{73}$$

$$R_{t,s}^{retail,power} = \pi_t^{PBDR} \times \left(PD_{t,s}^{initial} + \Delta L_{t,s}^{PBDR}\right) - C_{t,s}^{IBDR} \quad \forall t \epsilon \Omega_T,\ s \epsilon \Omega_S \tag{74}$$

$$R_t^{retail,NG} = \pi_t^{retail,NG} \times GD_t \quad \forall t \epsilon \Omega_T \tag{75}$$

$$R_t^{retail,Heat} = \pi_t^{retail,Heat} \times HD_t \quad \forall t \epsilon \Omega_T \tag{76}$$

$$Cost_{t,s}^{Units} = \left(\sum_{dg \epsilon \Omega_{DG}} C_{dg,t,s} + \sum_{chp \epsilon \Omega_{CHP}} C_{chp,t,s} + \sum_{ess \epsilon \Omega_{ESS}} C_{ess,t,s} + \sum_{ev \epsilon \Omega_{EV}} C_{ev,t,s}\right) + \left(\sum_{boiler \epsilon \Omega_{Boiler}} C_{boiler,t,s} + \sum_{hss \epsilon \Omega_{HSS}} C_{hss,t,s}\right) \quad \forall t \epsilon \Omega_T,\ s \epsilon \Omega_S \tag{77}$$

The problem's second objective function is divided into three parts: the quantity of CO_2 emitted from buying energy from the upstream network, the CO_2 produced by the MEVPP units, and the CO_2 absorbed by the P2G, which are given in Equation (78). The amount of pollution caused by purchasing energy from the day-ahead electricity, thermal, and natural gas markets is shown in Equation (79). Equation (80) shows the amount of carbon dioxide produced by the DG, CHP, and boiler units. Equation (81) shows the amount of carbon dioxide absorbed by P2G [24].

$$f_2 = \min \sum_{s \epsilon \Omega_S} Prob_s \sum_{t \epsilon \Omega_T} \left(E_{t,s}^{Grid} + E_{t,s}^{Units} - E_{t,s}^{P2G}\right) \tag{78}$$

$$E_{t,s}^{Grid} = E_{t,s}^{Power} + E_{t,s}^{NG} + E_{t,s}^{Heat} \quad \forall t \epsilon \Omega_T,\ s \epsilon \Omega_S \tag{79}$$

$$E_{t,s}^{Units} = \sum_{dg \epsilon \Omega_{DG}} E_{dg,t,s} + \sum_{chp \epsilon \Omega_{CHP}} E_{chp,t,s} + \sum_{boiler \epsilon \Omega_{Boiler}} E_{boiler,t,s} \quad \forall t \epsilon \Omega_T,\ s \epsilon \Omega_S \tag{80}$$

$$E_{t,s}^{P2G} = \sum_{p2g \epsilon \Omega_{P2G}} E_{p2g,t,s} \quad \forall t \epsilon \Omega_T,\ s \epsilon \Omega_S \tag{81}$$

2.11 | Equality constraints

In MEVPP, the amount of generation and consumption of different energy sectors should be equal, as shown in Equations (82)–(85). Equations (82), (84), and (85) show equal constraints for electricity, natural gas, and heat, respectively. In Equation (83), the electricity load is calculated after implementing demand response programs.

$$\sum_{dg \epsilon \Omega_{DG}} P_{dg,t,s} + \sum_{chp \epsilon \Omega_{CHP}} P_{chp,t,s} + \sum_{ess \epsilon \Omega_{ESS}} \left(P_{ess,t,s}^{dch} - P_{ess,t,s}^{ch}\right) + \sum_{ev \epsilon \Omega_{EV}} \left(P_{ev,t,s}^{dch} - P_{ev,t,s}^{ch}\right) = P_{t,s}^{DA} + PD_{t,s} + P_{t,s}^{CC} \quad \forall t \epsilon \Omega_T,\ s \epsilon \Omega_S \tag{82}$$

$$PD_{t,s} = PD_{t,s}^{initial} + \Delta L_{t,s}^{PBDR} - \sum_{b \epsilon \Omega_B} \Delta L_{t,b,s}^{IBDR} \quad \forall t \epsilon \Omega_T,\ s \epsilon \Omega_S \tag{83}$$

$$\sum_{p2g \epsilon \Omega_{P2G}} G_{p2g,t,s} = G_{t,s}^{DA} + \sum_{dg \epsilon \Omega_{DG}^{gas\_fired}} F_{dg,t,s} + \sum_{chp \epsilon \Omega_{CHP}} F_{chp,t,s} + \sum_{boiler \epsilon \Omega_{Boiler}} F_{boiler,t,s} + GD_t \quad \forall t \epsilon \Omega_T,\ s \epsilon \Omega_S \tag{84}$$

$$\sum_{chp \epsilon \Omega_{CHP}} H_{chp,t,s} + \sum_{pvt \epsilon \Omega_{PVT}} H_{pvt,t,s} + \sum_{boiler \epsilon \Omega_{Boiler}} H_{boiler,t,s} + \sum_{hss \epsilon \Omega_{HSS}} H_{hss,t,s} \quad \forall t \epsilon \Omega_T,\ s \epsilon \Omega_S \tag{85}$$

2.12 | Market constraints

The simulated MEVPP can participate in the day-ahead electricity, natural gas, thermal energy, and electrical spinning reserve markets. Equations (86)–(88) show the exchange of energy with the electricity, natural gas, and thermal energy markets. Equations (89)–(94) also show the maximum and minimum tradable power of these markets. Equations (95)–(97) prevent the simultaneous buying and selling of energy. The amount of pollution produced due to the purchase from the upstream network is calculated in Equations (98)–(100). Finally, Equation (101) determines the capacity of MEVPP units to participate in the electrical spinning reserve market.

$$P_{t,s}^{DA} = P_{t,s}^{DA,sell} - P_{t,s}^{DA,buy} \quad \forall t \epsilon \Omega_T,\ s \epsilon \Omega_S \tag{86}$$

$$G_{t,s}^{DA} = G_{t,s}^{DA,sell} - G_{t,s}^{DA,buy} \quad \forall t \epsilon \Omega_T,\ s \epsilon \Omega_S \tag{87}$$

$$H_{t,s}^{DA} = H_{t,s}^{DA,sell} - H_{t,s}^{DA,buy} \quad \forall t \in \Omega_T,\ s \in \Omega_S \tag{88}$$

$$0 \le P_{t,s}^{DA,buy} \le P^{DA,max} \times u_t^{power,buy} \quad \forall t \in \Omega_T,\ s \in \Omega_S \tag{89}$$

$$0 \le P_{t,s}^{DA,sell} \le P^{DA,max} \times u_t^{power,sell} \quad \forall t \in \Omega_T,\ s \in \Omega_S \tag{90}$$

$$0 \le G_{t,s}^{DA,buy} \le G^{DA,max} \times u_t^{NG,buy} \quad \forall t \in \Omega_T,\ s \in \Omega_S \tag{91}$$

$$0 \le G_{t,s}^{DA,sell} \le G^{DA,max} \times u_t^{NG,sell} \quad \forall t \in \Omega_T,\ s \in \Omega_S \tag{92}$$

$$0 \le H_{t,s}^{DA,buy} \le H^{DA,max} \times u_t^{heat,buy} \quad \forall t \in \Omega_T,\ s \in \Omega_S \tag{93}$$

$$0 \le H_{t,s}^{DA,sell} \le H^{DA,max} \times u_t^{heat,sell} \quad \forall t \in \Omega_T,\ s \in \Omega_S \tag{94}$$

$$u_t^{power,buy} + u_t^{power,sell} \le 1 \quad \forall t \in \Omega_T \tag{95}$$

$$u_t^{NG,buy} + u_t^{NG,sell} \le 1 \quad \forall t \in \Omega_T \tag{96}$$

$$u_t^{heat,buy} + u_t^{heat,sell} \le 1 \quad \forall t \in \Omega_T \tag{97}$$

$$E_{t,s}^{power} = \mu^{CO_2,power} \times P_{t,s}^{DA,buy} \quad \forall t \in \Omega_T,\ s \in \Omega_S \tag{98}$$

$$E_{t,s}^{NG} = \mu^{CO_2,NG} \times G_{t,s}^{DA,buy} \quad \forall t \in \Omega_T,\ s \in \Omega_S \tag{99}$$

$$E_{t,s}^{heat} = \mu^{CO_2,heat} \times H_{t,s}^{DA,buy} \quad \forall t \in \Omega_T,\ s \in \Omega_S \tag{100}$$

$$P_{t,s}^{res} = \sum_{dg \in \Omega_{DG}} Res_{dg,t,s} + \sum_{chp \in \Omega_{CHP}} Res_{chp,t,s} + Res_{t,s}^{IBDR} \quad \forall t \in \Omega_T,\ s \in \Omega_S \tag{101}$$

The complete procedure of solving the optimization is shown schematically in Figure 4. As seen in this figure, the load and market price parameters for thermal energy and natural gas are assumed deterministic, and the other parameters are considered stochastic.

3 | UNCERTAINTY MODELING AND MULTI OBJECTIVE OPTIMIZATION

The energy management system (EMS) should consider all possible scenarios of the uncertain parameters for optimal scheduling of MEVPP. The output power of RES such as WT, PV, and PVT is highly dependent on weather conditions. Other uncertain parameters include electricity consumption and market price, which depend on the behaviour of consumers and market participants, respectively. Also, the distance travelled during the day, the time of entering and leaving the parking lot in electric vehicles are some of the uncertainties that depend on the behaviour of vehicle drivers [29]. These parameters increase the uncertainty of the problem, which can be covered by generating scenarios. The scenario generation method for each uncertain parameter is described in the following.

3.1 | Electric vehicles

Scenario generation for EVs consists of obtaining probability density functions (PDF), scenario generation, and assigning battery information to each vehicle. In the first part, data related to the behaviour of EV drivers are extracted from [35]. The behaviour of EV drivers includes the distance travelled during the trip, the arrival time, and the departure time from the parking lot. It is also assumed that any EV can only have one trip during the day. Then, using the distribution fitter tool in MATLAB software, the gamma, Weibull, and generalized extreme value (GEV) functions are obtained for the departure time, arrival time, and the distance travelled during the trip, respectively. In the second part, using the obtained PDF, 20,000 scenarios are generated for each parameters. The generated scenarios are reduced to 200 using the K-means method to reduce the computational burden of the problem. Among the remaining scenarios, a few scenarios contain incorrect information. After deleting these scenarios, 109 scenarios remain. Finally, in the last part, using the information of reference [32], values of battery capacity, charge rate, and the electrical energy consumption per mile are randomly assigned to each of the EVs. A schematic of the scenario generation process for EVs is shown in Figure 5.

3.2 | Other parameters

Other uncertainty parameters include electricity demand, wind speed, solar radiation, and electricity market price, for which the normal, Weibull, Beta, and Normal PDF functions are assumed, respectively [4]. First, 1000 scenarios for each uncertainty parameter are generated using the mentioned PDF. The generated scenarios are then reduced to 7 scenarios using the Backward method [36]. The reduced scenarios are mixed together, and 2401 scenarios are obtained. The number of mixed scenarios is high, which increases the computational burden of the problem. Therefore, the mixed scenarios are reduced to 7 scenarios using the Backward method and applied to the optimization problem. According to the Backward method, first, the Kantorovich distance between the scenarios in the original set is calculated. Then, scenarios with similar Kantorovich distances and low probability are removed from the original set in an iterative process until the desired number of scenarios remains [36].

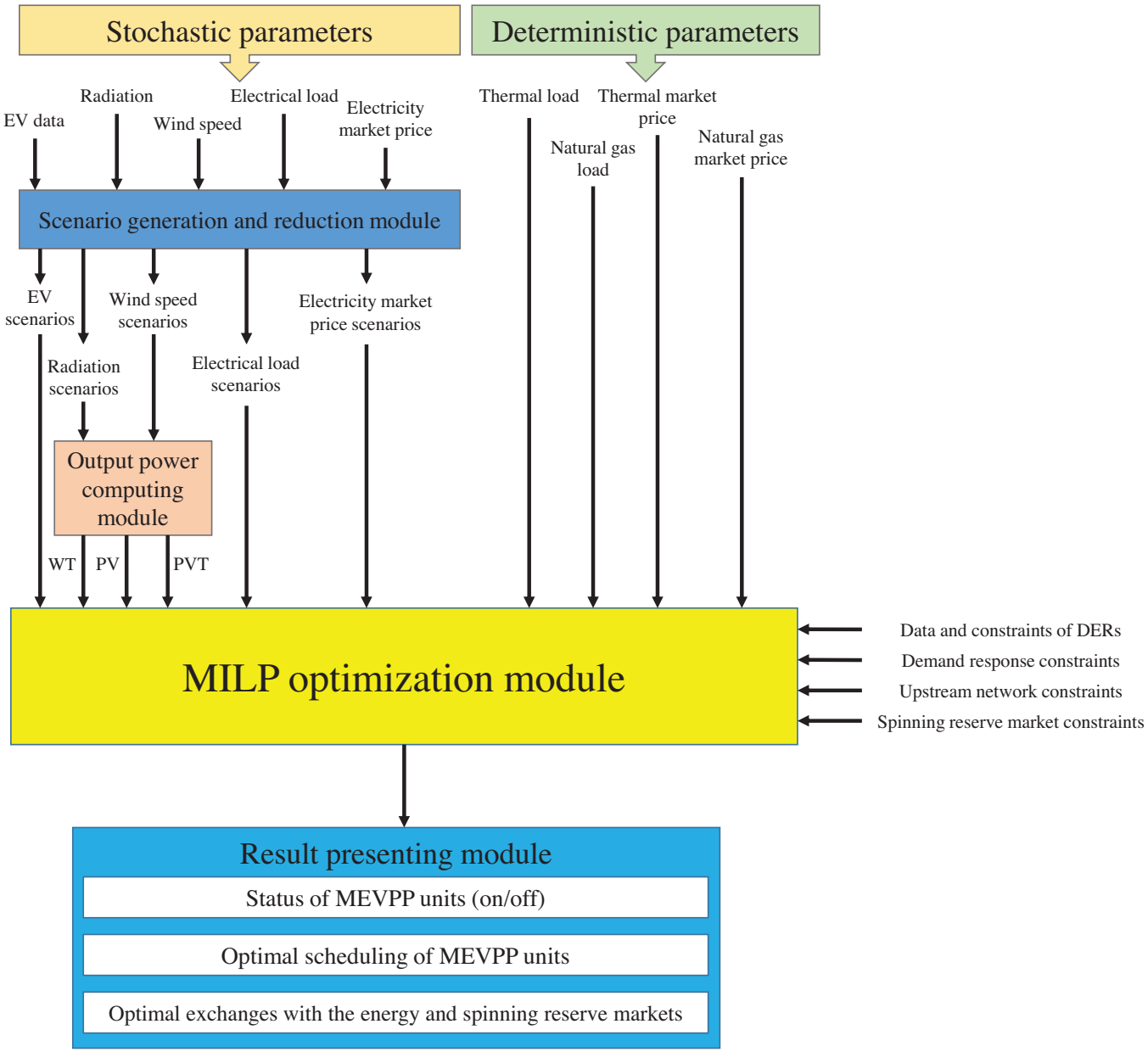

FIGURE 4 Complete procedure of solving optimization problem

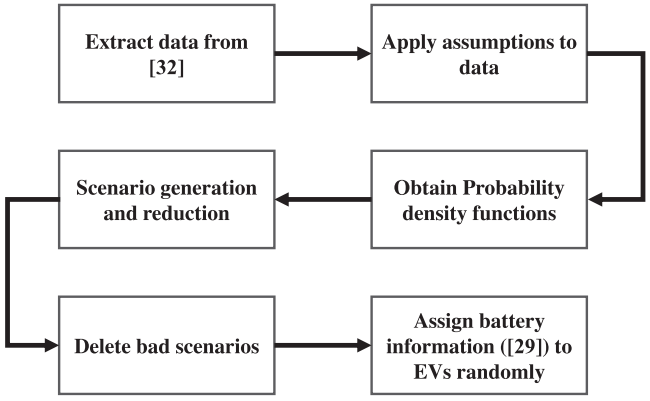

FIGURE 5 The uncertainty modelling process for EVs

The problem has two objective functions of maximizing the profit of MEVPP and minimizing the amount of emission, which are in conflict with each other. Therefore, to make a trade-off between these objective functions, it is necessary to solve the problem as a multi-objective problem. In this paper, the Epsilon constraint method is used for multi-objective optimization. In this method, one of the objective functions is optimized as the main objective function of the problem, and other objective functions are added to the problem as a constraint. The MEVPP profit maximization is considered as a main objective function, while emission minimization is considered as a constraint [37, 38]. The formulation of the model is summarized below.

$$\begin{gathered}\max f_1 \\ \text{subject. to}: f_2 \le \varepsilon \\ \text{other constraints}\end{gathered} \tag{102}$$

In (102), the amount of Epsilon varies between the minimum and maximum values of the second objective function (emission minimization). These values are obtained through the payoff table described in [39]. The optimization problem is then solved multiple times, and each time, the Epsilon value varies. Therefore, Pareto points are obtained as solutions to the multi-objective problem.

The decision-maker tries to find the best compromise solution between Pareto points, which can be achieved using the fuzzy satisfying method. In this method, the values of the objective functions at each Pareto point are normalized using fuzzy membership functions between zero and one. The closer the fuzzy number is to one, the more successful the Pareto point is at optimizing the objective function. Given that the two objective functions of the problem conflict with each other, if the fuzzy number of one objective function gets closer to 1, the other objective function's fuzzy number will approach zero. As a result, a Pareto point with an acceptable fuzzy number must be chosen for both objective functions. First, the fuzzy numbers of each objective function are calculated using Equations (103) and (104). Then the minimum values are chosen between the fuzzy numbers of the two objective functions, and finally, the decision-maker selects the maximum value from the minimum values (Equation (105)) [40, 41].

$$\mu_1^p = \begin{cases} \dfrac{f_1^p - f_1^{min}}{f_1^{max} - f_1^{min}} & f_1^{min} \le f_1^p \le f_1^{max} \\ 0 & otherwise \end{cases} \tag{103}$$

$$\mu_2^p = \begin{cases} \dfrac{f_2^{max} - f_2^p}{f_2^{max} - f_2^{min}} & f_2^{min} \le f_2^p \le f_2^{max} \\ 0 & otherwise \end{cases} \tag{104}$$

$$\max_p \left(min\left(\mu_1^p, \mu_2^p\right)\right) \tag{105}$$

4 | NUMERICAL RESULTS

4.1 | Input data

Figures 6 and 7 depicts the MEVPP, which comprises electrical, thermal, and natural gas demands. Figure 1 also depicts the MEVPP's generation units. The MEVPP mentioned above can engage in the day-ahead electricity, thermal, natural gas, and spinning reserve electricity markets to increase its profit and provide its loads. The maximum amount of power that can be exchanged with upstream electrical and thermal networks is 1000 kW, and with natural gas network is 5000 MBTU. Other information about the MEVPP is given below:

- Climatic data, such as wind speed, solar radiation, ambient temperature, and specifications for WT, PV, and PVT power plants, are extracted from reference [4].
- The data about the day-ahead market prices, including the electricity, thermal, and natural gas markets, is taken from references [4, 27], and the spinning reserve market price according to reference [30] is equal to 30% of the day-ahead electricity market price.
- The retail electricity price is 0.1216 $/kWh. This price is the TOU program's average pricing on 30 August, 2021 [42]. Furthermore, according to [43], the retail price of natural gas to customers in 2020 is 0.01084 $/MBTU, and the retail price of thermal energy is 0.080 $/kWh [4].
- Technical and economic specifications of all units are given in Table 3 [21, 30, 44, 45].
- Electric vehicle requirements, such as distance travelled, arrival time, and departure time from the parking lot, are handled using the scenario generation method mentioned in Section 3.1, and specifications for electric vehicle batteries are taken from reference [32].
- Consumer participation in DR programs is considered 10%. In the IBDR program, which includes three price levels, each level has a 20% increase in price compared to the previous level, and the cost of the first level is equal to 0.05 $/kWh [7], and RTP pricing method has also been employed in PBDR programs [33].
- The heat value of natural gas is 2.7983 MBTU/kWh [30].
- The mean is equal to the predicted data in the normal distribution function, and the standard deviation equals 10% of the mean. In the beta distribution function, the alpha and beta values are calculated after determining the mean and standard deviation in the same way. In the Weibull distribution function, the value of the scale parameter is $\sqrt{2}/\pi$ times the predicted data, and the shape parameter is equal to 5.

4.2 | Simulation results

MEVPP is modelled as a multi-objective problem with the objectives of maximizing profits and minimizing emissions. In this section, the VPP's stochastic optimization problem is represented by taking into account uncertain parameters such as electric demand, day-ahead electricity market price, solar radiation, wind speed, and the behaviour of electric vehicle drivers. Seven scenarios are considered for the mentioned uncertainties, and the most probable scenario is reported as the simulation results. In the interchange of MEVPP with energy markets, it is assumed that a negative amount is equal to buying from the market, and a positive amount is equal to selling to the market. About storage devices, it is also assumed that a positive value is equal to the amount of discharge and a negative value is equal to the amount of charge. The following two cases are considered to evaluate the advantages of MEVPP over VPP, and each will be addressed in detail below.

- Modelling the optimal scheduling problem for a VPP

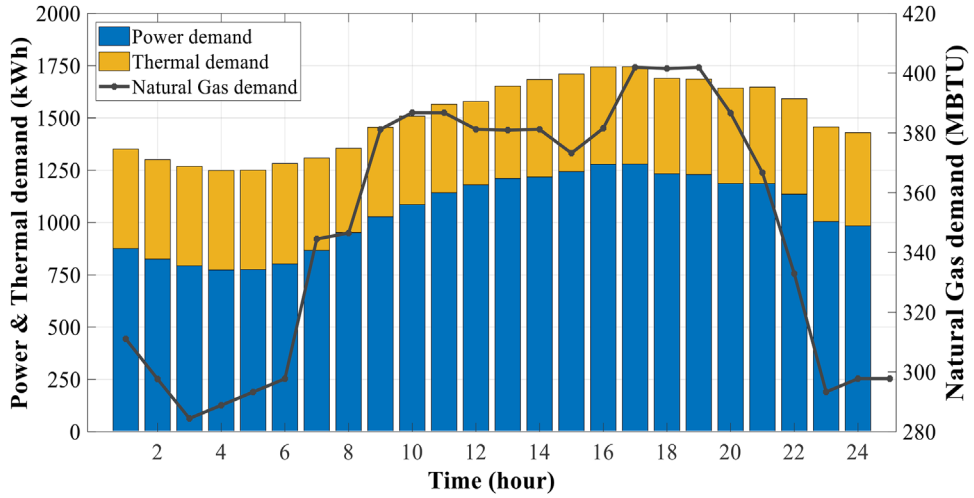

FIGURE 6 Electric, thermal, and natural gas demand of the MEVPP

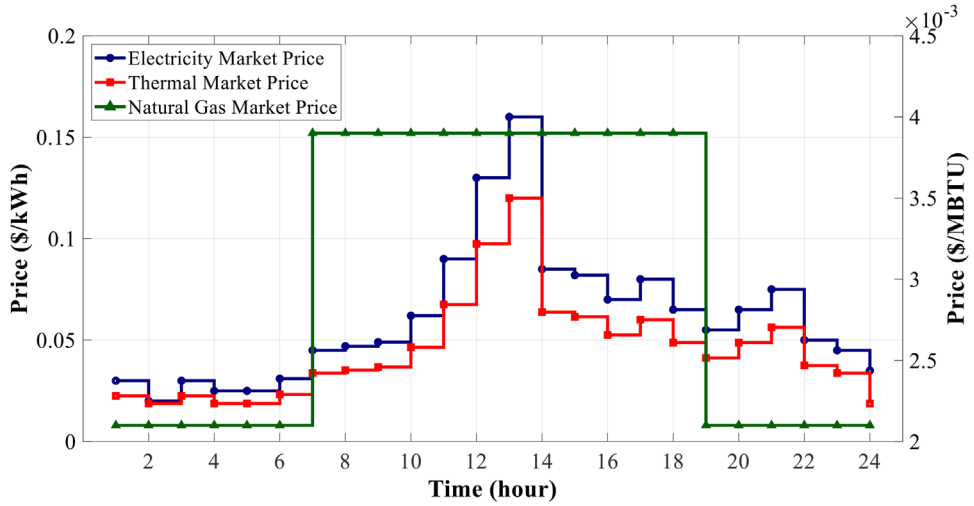

FIGURE 7 The electricity, thermal and natural gas markets prices

- Modelling the optimal scheduling problem for MEVPP

The proposed model is an MILP model implemented in GAMS and solved using a CPLEX solver. This simulation was done on a system with 8GB RAM and a 2.4 GHz CPU. The simulation results are analysed in the following sections.

4.2.1 | Case 1

In this case, a VPP that includes electrical energy resources is modelled. The VPP includes MT, FC, ESS, and EV units and can participate in day-ahead and spinning reserve markets. This case is similar to the proposed model that has been introduced in [8, 23, 26]. Comparing the results of this case with Case 2 proves the need for MEVPP modelling.

The optimal VPP scheduling problem is solved in this case for profit maximization, pollution minimization, and multi-objective optimization, as shown in Table 4. It should be noted that the most probable scenario is reported. Also, the best Pareto point is selected as the final result in the multi-objective optimization case. As given in Table 4, VPP profits are derived from market exchanges and electricity sales to consumers. VPP profits have the highest and lowest quantity in profit maximization and pollution minimization, respectively. This is also true for the pollution produced. Thus, the amount of pollution in the profit maximization case is 1.31 times the amount of pollution in the case of pollution minimization. As a result, multi-objective optimization can be used to make a trade-off between profit and pollution.

Figure 8 shows the VPP's interaction with the day-ahead and spinning reserve markets in a multi-objective case. Due to the high emission factor of the upstream network, the VPP has not

TABLE 3 Specifications of MEVPP generation units

Parameter	Value	Parameter	Value	Parameter	Value	Parameter	Value
$a^{dg\#1}$	0.04	$\mu^{dg\#2}$	0.32	η^{chp}	0.3	H^{max}_{boiler}	200
$b^{dg\#1}$	0.85	$a^{dg\#3}$	0.03	μ^{chp}	0.72	η^{boiler}	0.85
$SUC^{dg\#1}$	0.09	$b^{dg\#3}$	2.5	a_{ess}	0.008	μ^{boiler}	0.51
$SDC^{dg\#1}$	0.08	$SUC^{dg\#3}$	0.16	b_{ess}	0.01	P^{min}_{p2g}	0
$P^{dg\#1}_{min}$	90	$SUC^{dg\#3}$	0.09	$P^{ch/dch,min}_{ess}$	20	P^{max}_{p2g}	80
$P^{dg\#1}_{max}$	900	$P^{dg\#3}_{min}$	60	$P^{ch/dch,max}_{ess}$	200	$G^{ch/dch}_{p2g,min}$	0
$RU^{dg\#1}$	360	$P^{dg\#3}_{max}$	600	SOC^{min}_{ess}	100	$G^{ch/dch}_{p2g,max}$	1412
$RD^{dg\#1}$	360	$RU^{dg\#3}$	240	SOC^{max}_{ess}	1000	GS^{min}_{p2g}	1412
$\eta^{dg\#1}$	0.35	$RD^{dg\#3}$	240	$SOC_{ess,t0}$	200	GS^{max}_{p2g}	7060
$\mu^{dg\#1}$	0.32	$\eta^{dg\#3}$	0.5	η^{ess}	0.9	$GS_{p2g,t0}$	2118
$a^{dg\#2}$	0.01	$\mu^{dg\#3}$	0.21	a_{hss}	0.001	η^{p2g}	0.75
$b^{dg\#2}$	6.5	$[H^A_{chp}, P^A_{chp}]$	[0, 247]	b_{hss}	0.01	$\eta^{ch/dch}_{p2g}$	0.95
$SUC^{dg\#2}$	0.09	$[H^B_{chp}, P^B_{chp}]$	[180, 210]	$H^{ch/dch,min}_{hss}$	0	μ^{p2g}	1.35
$SDC^{dg\#2}$	0.08	$[H^C_{chp}, P^C_{chp}]$	[105, 81]	$H^{ch/dch,max}_{hss}$	160	$\mu^{CO_2,power}$	0.92
$P^{dg\#2}_{min}$	70	$[H^D_{chp}, P^D_{chp}]$	[0, 98]	SOC^{min}_{hss}	0	$\mu^{CO_2,NG}$	0.05307
$P^{dg\#2}_{max}$	700	RU^{chp}	110	SOC^{max}_{hss}	480	$\mu^{CO_2,heat}$	0.921
$RU^{dg\#2}$	280	RD^{chp}	110	$SOC_{hss,t0}$	96	η^{CC}	0.9
$RD^{dg\#2}$	280	SUC^{chp}	0.22	η^{hss}	0.9	ρ^{CC}	0.12
$\eta^{dg\#2}$	0.3	SDC^{chp}	0.09	H^{min}_{boiler}	0		

$dg\#1,2 = non-gas\ fired$, $dg\#3 = fuel\ cell\ (gas-fired)$.

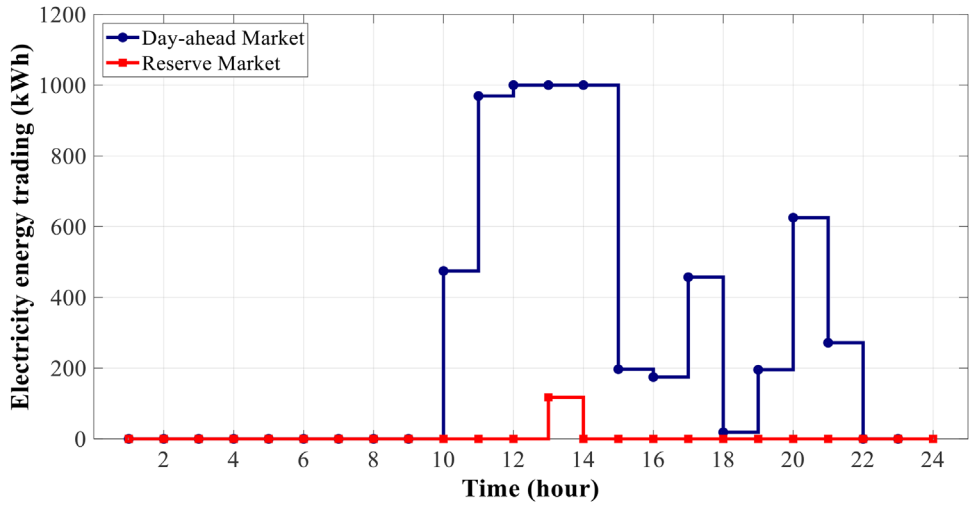

FIGURE 8 The amount of energy interchange of VPP with energy markets

purchased power from the day-ahead market at any time of day, as shown in Figure 8. In contrast, when the market price is high, it has sold its power to the upstream network to increase its profit. Because the spinning reserve market price is equal to 30% of the day-ahead market, VPP participates in this market only at hour 13, when the market price is high.

Figure 9 shows the generated power of VPP units. According to this figure, the DG3 generates all-day hours due to its lower emission factor. The DG2 also generates most of the day due to its low operating costs. In contrast, DG1 generates power in a few hours of the day due to its high operating costs. As shown in Figure 9, the ESS unit is charged when the market price is low and discharged during the hour when the market price is high. EVs behave similarly to ESS. It should be noted that EVs are often parked in the parking lot in the early and last hours of the day, so they are charged during these hours.

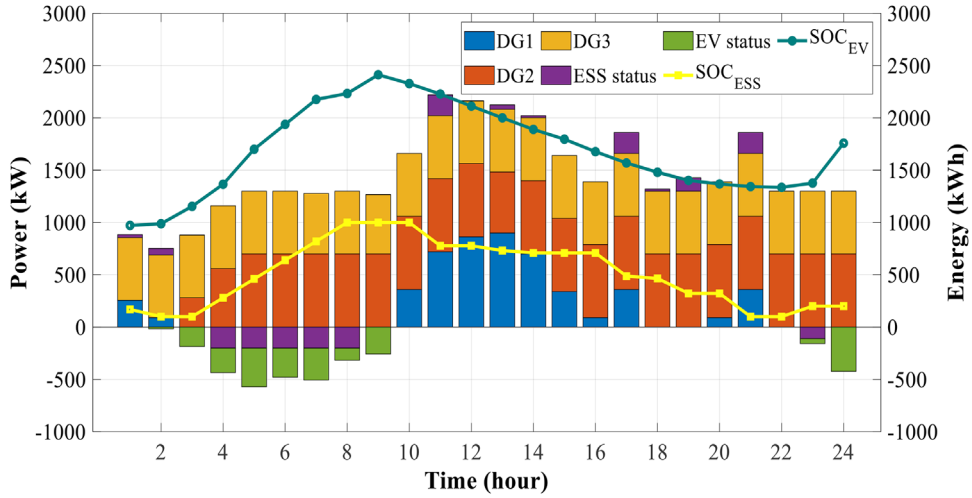

FIGURE 9 The amount of electrical energy generation of VPP units

TABLE 4 Simulation results for single-objective and multi-objective cases of VPP

	Max profit	Min emission	Multi-objective
f_1	3039.64	2221.694	2825.91
f_2	15,683.85	6728.65	9415.209
$R^{power,DA}$	1048.544	0	626.6502
$R^{power,res}$	4.467338	0	5.458081
$R^{retail,power}$	3084.421	3084.421	3084.421
C_{dg}	1243.769	891.7051	997.4578
C_{ESS}	2.11	0	2.311111
C_{EV}	−159.5344	−37.57926	−111.8582
E^{power}	4139.676	0	0
E^{Units}	11,448.79	6773.404	9364.934

4.2.2 | Case 2

In this case, an MEVPP including electric, thermal, and natural gas resources is modelled, and its structure is depicted in Figure 1. Table 5 provides the MEVPP simulation results as single-objective and multi-objective cases. If the MEVPP's objective function is to maximize profit, the amount of pollution will be extremely large. Furthermore, if the MEVPP's objective function is to minimize pollution, its profit will be significantly reduced. To address this issue, we employ multi-objective optimization to find the best points for both objective functions. The Epsilon constraint method generated 30 Pareto points, as shown in Figure 10, and the most conservative point was chosen as the best Pareto point.

The RTP program has also been deployed to encourage higher customer participation and maximum load shifting. According to reference [14], the RTP method has a stronger influence on flattening the load profile and enhancing the MEVPP's profit than other pricing methods such as FP and TOU. As mentioned in the results of Table 5, in a multi-objective case, the profit of the MEVPP is equal to 3977.86 $, and the amount of emission production is equal to 7174.36 kg. The MEVPP earns profit through interacting with the energy markets and selling electricity to consumers. Also, due to the lack of natural gas generation units and dependency of P2G on weather conditions, the MEVPP operator always participates in the natural gas market as a buyer and always has a negative profit. As a result, it tries to get the natural gas it needs from the upstream network at the lowest cost.

In Table 5, according to the emission produced by the upstream networks, the amount of energy purchased from that network can be achieved. According to Table 5, the amount of energy purchased from upstream networks has decreased compared to the maximizing profit case. Because energy purchases from upstream networks have a high emission factor, so the MEVPP has tried to rely on its generation units to reduce emission and only buy the energy it needs from the upstream network when necessary. Figure 11 depicts the MEVPP's energy interchange with energy markets. According to Figure 11, the MEVPP has sold its energy when the price of energy markets is high, and it will buy energy if necessary when the price of energy markets is low. According to the total cost of energy storage, shown in Table 5, the use of these units has increased due to their low operating costs and lack of emission compared to the situation where the problem is solved to maximize profits.

Also, the P2G unit generates more natural gas in the multi-objective case than other cases, which reduces the cost of purchasing natural gas and significantly reduces emissions. In general, in this case, the MEVPP operator, with proper planning of units, has been able to optimize the objective functions of maximizing the profit and minimizing the emission production simultaneously.

Figure 12 shows the daily generation of each electricity unit. DG1 is the most expensive generation unit among the DG units, and DG2 is the cheapest unit. On the other hand, DG1 and DG2 are non-gas fired units and DG3, a fuel cell, is a gas-fired unit. DG1, the largest generation unit of all DGs, is on

TABLE 5 Simulation results for single-objective and multi-objective cases of MEVPP

	Max profit	Min emission	Multi-objective		Max profit	Min emission	Multi-objective
f_1	4198.9	3000.83	3977.79	C_{chp}	121.76	13.09	70.44
f_2	16,863.72	4225.66	7174.54	C_{ESS}	2.09	3.20	2.71
$R^{power,DA}$	881.62	0	640.87	C_{EV}	−159.2	−37.6	−76.3
$R^{NG,DA}$	−223.9	−18.18	−90.86	C_{Boiler}	47.41	13.15	38.07
$R^{Heat,DA}$	379.38	−13.48	273.86	C_{HSS}	1.25	0.97	1.68
$R^{power,res}$	46.69	0	45.19	E^{power}	5634.27	0	0
$R^{retail,power}$	3189.04	2897.44	3182.22	E^{NG}	4022.49	396.92	1803.65
$R^{retail,NG}$	91.05	91.05	91.05	E^{Heat}	1205.67	2479.59	968.59
$R^{retail,Heat}$	868.61	868.61	868.61	E^{Units}	15,707.87	8932.77	14,216.09
C_{dg}	1020.42	804.64	1019.92	E^{P2G}	9084.41	7248.39	9593.78

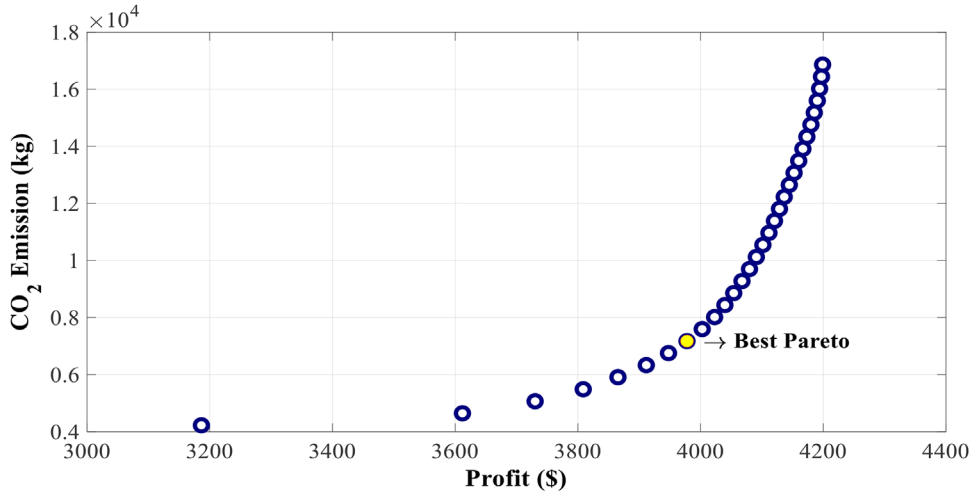

FIGURE 10 Set of Pareto optimal solutions using the Epsilon constraints method in multi-objective optimization

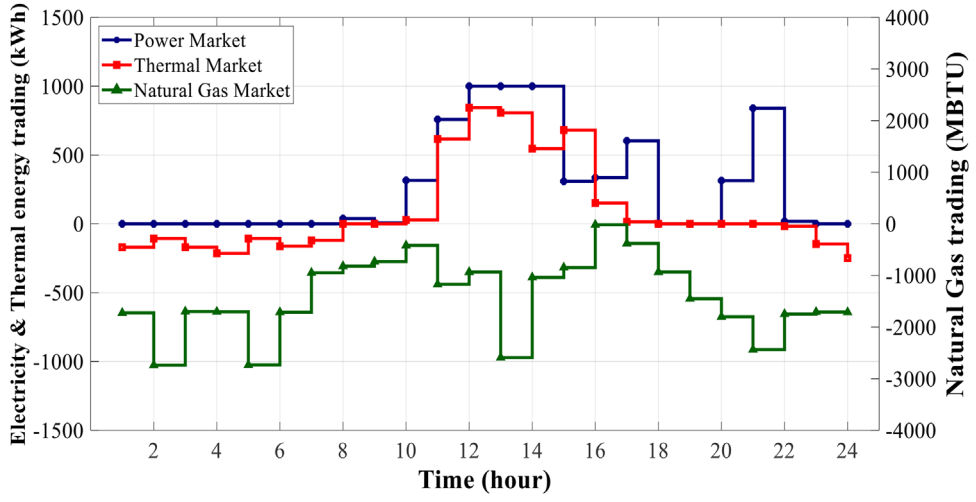

FIGURE 11 The amount of energy interchange of MEVPP with energy markets

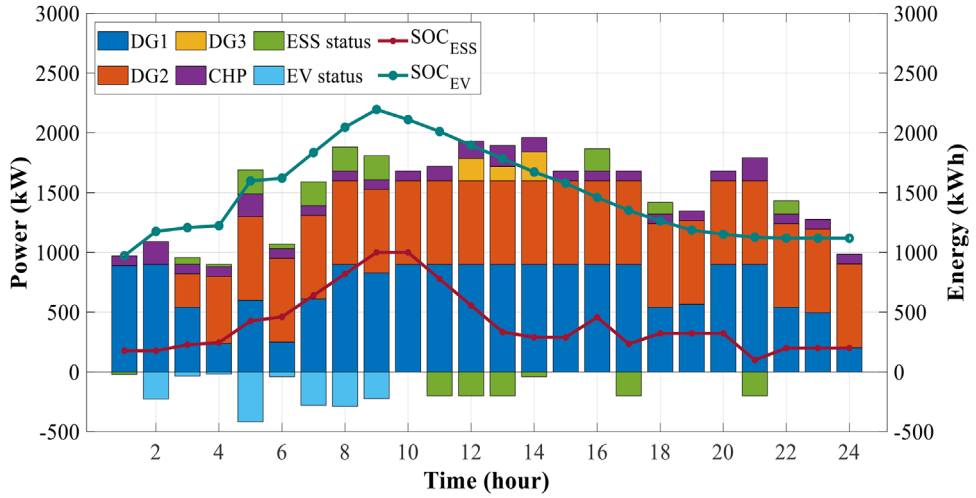

FIGURE 12 The amount of electrical energy generation of MEVPP units

at all hours of the day. Due to lower electricity demand during specific hours of the day, such as 3 to 7 and 22 to 24, this unit reduces its generation while still generating electricity at full capacity for the remainder of the day. In the first two hours of the day, DG2 is off according to (13). This unit turns on around 3 o'clock and operates at full capacity until the end of the day. DG3 has the lowest emission coefficient among other DGs; however, because it is a gas-fired unit, its electrical energy generation imposes a natural gas demand on the network. As a result, due to the maximum day-ahead market price, this unit only generates electricity to increase the MEVPP's profit from 12 to 14 and is off the rest of the day. The CHP unit was used at 2 and 5 to charge the electric vehicles' battery and compensate for the generation of DG2. Between 11 and 14 and 21, the CHP increased its generation due to rising day-ahead electricity market prices. The ESS charges from 3 to 9 due to the low price of the electricity market and the electricity load, and it discharges from 11 to 13 when the electricity market's price is high to increase the MEVPP's profit. Due to Equation (34), this unit charges at 22. Most electric vehicles are in the parking lot in the early and late hours of the day and can charge their batteries. Therefore, the electric load is inserted on the network when electric vehicles are charged. For this reason, electric vehicles charge their batteries during off-peak hours, such as 2 to 9.Due to the high cost of discharging the battery compared to other storage devices, the MEVPP operator prefers only to charge the batteries of electric vehicles. Therefore, the battery is discharged only during travel.

Figure 13 shows the amount of spinning reserve of MEVPP that have participated in the electricity spinning reserve market. DG1 unit has the highest operating cost among distributed generation units. Therefore, it is not economical for this unit to participate in the spinning reserve market. In contrast, because the DG2 is the cheapest unit among all DGs, it generates its total capacity at all hours of the day. The DG3 is a gas-fired unit that needs more fuel to increase its reserve capacity. This increases the natural gas demand. For this reason, DG units do not participate in the spinning reserve market. Because at 13 o'clock, the price of the spinning reserve market is at its maximum, the CHP unit has participated in this market. Interruptible loads also participate in the spinning reserve market most hours of the day and are ready to reduce loads if necessary.

Figure 14 shows the changes in the electrical load of an MEVPP after the implementation of DR programs. After implementing the RTP program, electrical energy consumption increased during the off-peak hours and decreased during the peak hours. As shown in the figure, this program makes the load profile smoother and increases the load factor. Interruptible loads are another DR program in this article. At 1, 23, and 24 h, the interruptible loads of the MEVPP have decreased. In fact, during these hours, the cost of reducing the load is less than generating power by expensive units. Especially at 1 o'clock, due to the minimum off-time constraint of DG2, reducing the load is preferred to increasing the generation of other units. Because of the increase in the day-ahead electricity market price, the MEVPP operator at 11, 17, and 21 have decided to reduce the loads to optimize their profit. However, in other hours when the electricity market price is high, the load is not reduced due to Equation (90). According to this constraint, the MEVPP interchange its maximum energy with the upstream network, and even if the load is reduced, it cannot interchange more energy with its upstream network.

Figure 15 shows the amount of thermal energy generation of MEVPP units. The boiler is the most cost-effective way to generate thermal energy. As a result, this unit has been utilized to supply thermal loads at all hours of the day. Thermal load rises from 1 to 8 and 19 to 24, whereas thermal market price rises from 11 to 15. For this reason, CHP and boiler units increase their generation to their maximum heat capacity. PVT is one of the most important units for generating thermal energy without producing any pollution. From 08:00 AM to 07:00 PM, this unit begins generating thermal energy in accordance to the sun's radiation. Furthermore, the day-ahead thermal market price is high during these hours, increasing the MEVPP's interchange

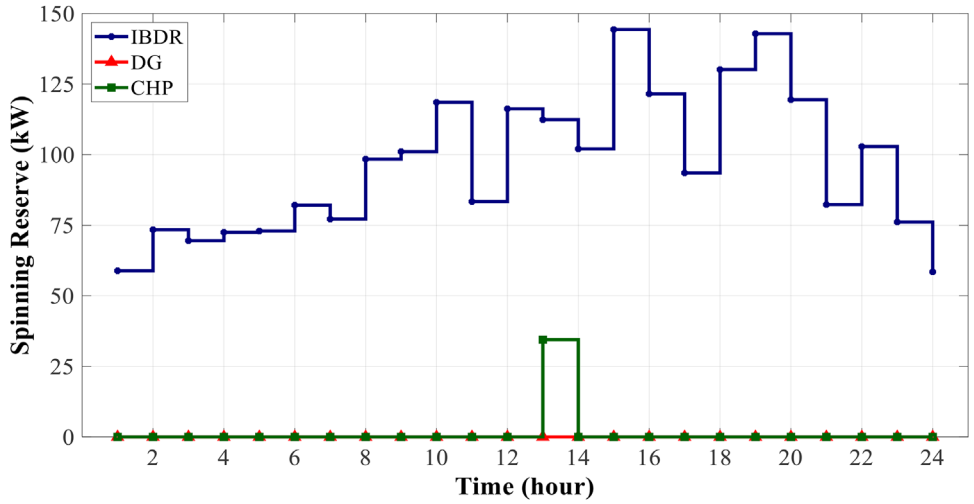

FIGURE 13 The amount of reserve capacity of MEVPP units to participate in the spinning reserve market

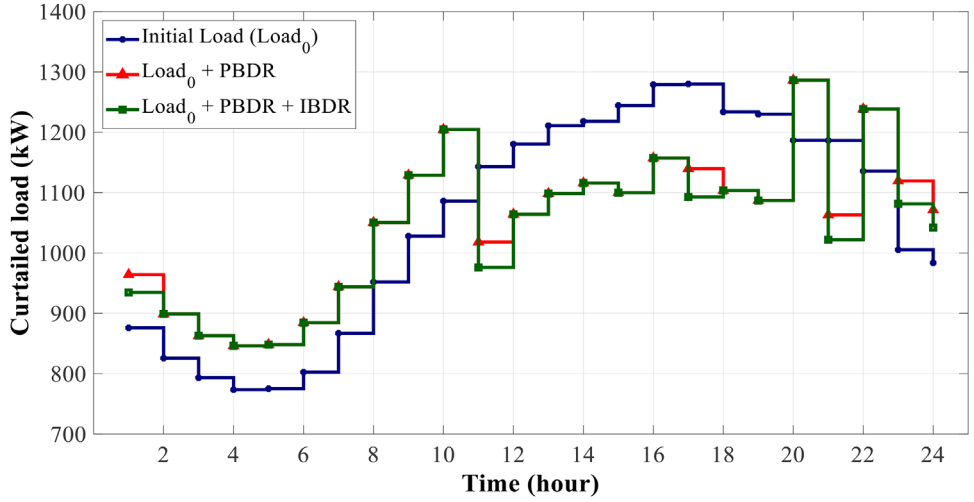

FIGURE 14 MEVPP electrical load changes after the implementation of PBDR and IBDR programs

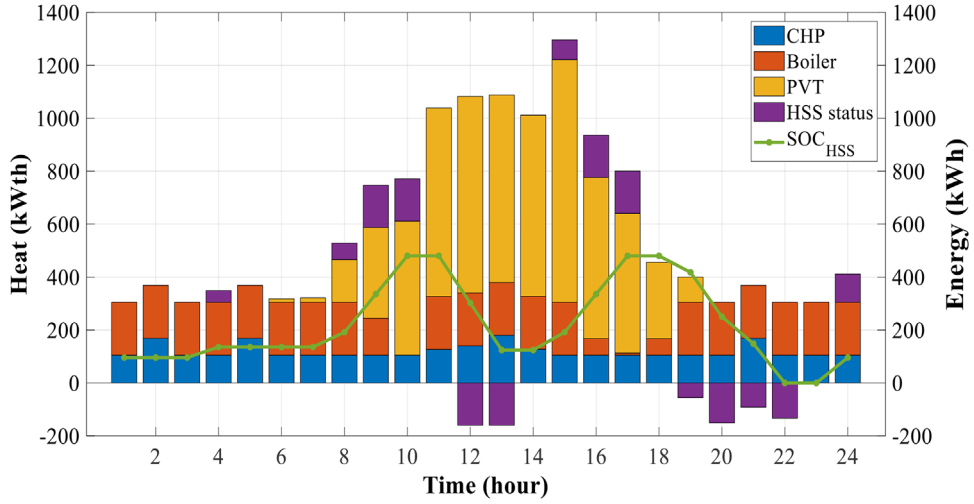

FIGURE 15 The amount of thermal energy generated by each of the MEVPP units

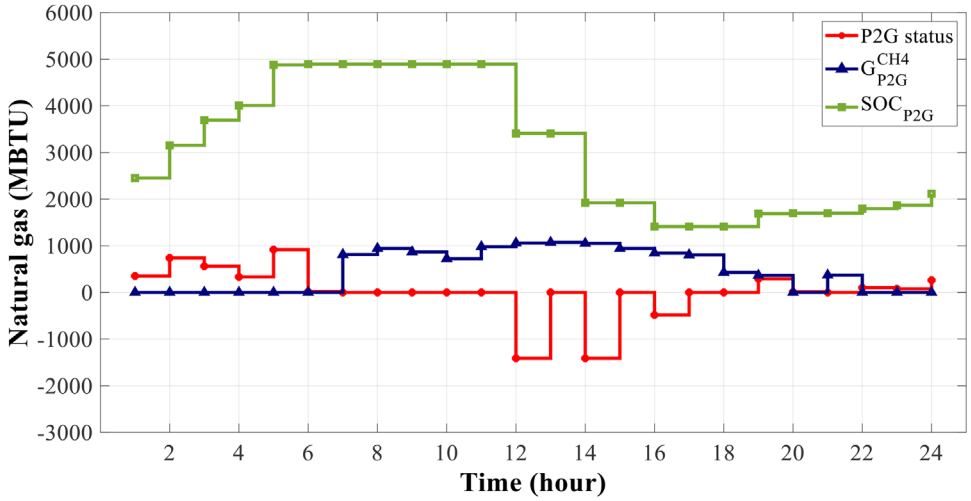

FIGURE 16 Natural gas generation by P2G unit

with the upstream network and increasing the MEVPP's profit. The HSS is charged between 8 and 10 due to low consumption and market price. In addition, because of the high generation of the PVT, this unit is charged between 02:00 PM and 05:00 PM. Similarly, because of the high market price, this unit will discharge between 12:00 PM and 01:00 PM. Due to the high thermal load demand, HSS discharged from 07:00 PM to 10:00 PM.

Figure 16 depicts the P2G unit's natural gas generation as the MEVPP's sole natural gas producer. This unit stores natural gas in its tank from 1 to 5 due to an increase in wind speed, low natural gas market prices, and low consumption. In addition, due to the increase in the natural gas market price and the generation of electricity by DG3, it will release its stored natural gas at 01:00 PM and 02:00 PM to compensate for a portion of the costs of purchasing natural gas from the upstream network. The sun's radiation increases from 07:00 AM to 06:00 PM; hence this unit injects natural gas directly into the grid.

TABLE 6 Sensitivity analysis on the participation rate in demand response programs

	Participation rate in demand response programs				
Variables	**0**	**0.05**	**0.1**	**0.15**	**0.2**
f_1	3823.21	3901.4	3977.8	4056.8	4101.0
f_2	7680.63	7430.9	7174.5	6982.4	6359.2
P^{DA}	7756.90	7415.2	7357.4	7507.4	6986.0
P^{res}	117.38	1214.5	2355.5	3382.4	4014.1
G^{DA}	−43294.3	−38,825.1	−37,750.9	−34,757.9	−29,314.6
H^{DA}	2681.4	2709.9	2634.2	2401.3	2104.5
$P^{total,MEVPP}$	34,589.2	34,104.5	33,928.8	33,848.5	32,705.9
$G^{total,MEVPP}$	13,539	13,567.5	13,491.9	13,258.9	12,962.1
$H^{total,MEVPP}$	15,891.0	15,826.7	15,865.8	15,891.3	15,643.1
$E^{total,MEVPP}$	4379.8	4367.2	4257.9	4109.2	3765.4
$E^{upstream}$	3300.9	3063.7	2916.6	2873.3	2593.8
PD	25,225.5	25,087.9	24,978.7	24,762.5	24,194.5

4.3 | Sensitive analysis

This section performs a sensitive analysis on load participation rate (PR) in demand response programs. The PR determines what percentage of MEVPP loads participate in demand response programs. This parameter was assumed to be 10% in base case. Table 6 shows the results of the problem for different values of PRs. According to this table, with increasing PR, the amount of electricity demand and MEVPP participation in the spinning reserve market decrease and increase, respectively. This is because of the increased load curtailment capacity in the IBDR program. Generation of MEVPP units and interaction with energy markets has also decreased with increasing PR. As a result, the operation cost of these units is reduced. The decrease in the cost of MEVPP units and the increase in MEVPP's participation in the spinning reserve market have increased the overall profit of MEVPP. Additionally, reducing the generation of these units and MEVPP's interaction with the upstream network has resulted in less pollution.

5 | CONCLUSION

This paper investigated the optimal operation of VPP and MEVPP. The Epsilon constraint method was used to maximize profits while minimizing emissions. In addition, utilizing the Fuzzy satisfying approach, the best Pareto point was chosen as the optimal solution of the problem. The proposed MEVPP supplies electric, thermal, and natural gas loads by having various units. This power plant can interchange energy with the day-ahead energy markets like electricity, thermal, and natural gas. Also, the MEVPP participates in the electricity spinning

reserve market to increase its profit. In this study, PBDR and IBDR programs were implemented on the electrical loads of the MEVPP, which increased the load factor and smoothed the load profile. The scenario generation and reduction method was used to handle the uncertainties of electricity demand, electricity market price, wind speed, solar radiation, and the behaviour of electric vehicles. The simulation results demonstrated the performance of the MVPP scheduling model, as summarized below:

- The profit of MEVPP in multi-objective optimization mode has increased by 40.76% compared to VPP. Also, the amount of pollution produced by MEVPP compared to VPP has decreased by 23.79%.
- The total CO_2 produced by the MEVPP units and the upstream network is 16,988.33 kg, of which 9593.78 kg was absorbed by the P2G unit, resulting in a CO_2 reduction of 57.77%.
- Dispatchable units such as DG and CHP provide a significant amount of MEVPP demands due to their high capacity.
- Regarding energy market prices, energy storages enhances the flexibility and profitability of MEVPP.
- In addition to producing clean natural gas, P2G technology also reduces the cost of purchasing natural gas from the market using its storage tank.
- The presence of a PVT power plant, in addition to supplying the network's thermal load, has increased the MEVPP's profit in the day ahead thermal energy market.
- The RTP program raised the load factor by 2.03%. Also, the quantity of peak-to-valley has dropped from 506.35 kW to 398.26 kW, equivalent to 21.3%. The IBDR program also caused the MEVPP to participate its interruptible loads in the spinning reserve market during most of the day and increase the MEVPP's profit in this market.
- The sensitive analysis section also shows that with increasing the PR of electricity demand in demand response programs, the profit of MEVPP increases, and the amount of pollution produced also decreases.

The impact of energy transmission networks on MEVPP scheduling can be investigated in future works. Furthermore, emerging methods, such as neural networks, can better predict unexpected events in virtual power plants, which will be the subject of future research.

CONFLICT OF INTEREST

The authors have no conflicts of interest to declare. All co-authors agree with the contents of the manuscript and there is no financial interest to report. We certify that the submission is original work and is not under review at any other publication.

DATA AVAILABILITY STATEMENT

The data that support the findings of this study are available from the corresponding author upon reasonable request.

NOMENCLATURE

Indices

hss	Index of heat storage systems
b	Index of blocks
$boiler$	Index of boiler unit
chp	Index of combine heat and power unit
dg	Index of dg units
ess	Index of energy storage systems
ev	Index of electric vehicles
$p2g$	Index of P2G unit
pv	Index of photovoltaic panels
pvt	Index of PV-thermal panels
s	Index of scenario
t	Index of time (h)
wt	Index of wind turbine

Sets

$\Omega_{DG}, \Omega_{DG}^{gas\ fired}$	Sets of all distributed generations (DG), and gas fired DGs
$\Omega_{EV}, \Omega_{ESS}$	Sets of Electric vehicles (EV), and Energy storage systems (ESS)
Ω_{HSS}, Ω_{CHP}, Ω_{Boiler}	Sets of heat storage system (HSS), combined heat and power (CHP), and Boiler
Ω_{P2G}	Sets of power to gas (P2G)
Ω_S, Ω_B	Sets of scenarios, and blocks
Ω_T	Sets of time
$t^{parking}$	Times when electric cars are in the parking lot (h)
t^{trip}	Times when electric cars are in trip (h)

Parameters

$\{\cdot\}^{min}$, $\{\cdot\}^{max}$	Minimum/maximum limits of variables
CR_{EV}	Battery charge rate of EV (kW)
$EC_{EV,t}^{Trip}$	The amount of energy consumed during the trip by each EV (kWh)
$ECPM_{EV}$	Energy consumed per mile for each EV (kWh/mile)
GD_t, HD_t	Natural gas (MBTU)/Heat demand (kW)
$GS_{P2G,t0}$	Initial capacity of P2G gas tank (MBTU)
HV^{NG}	Natural gas heat value (MBTU/kW)
$H_{t,s}^{PVT}$	Thermal output of PVT (kW)
$Mileage_{EV,t}$	The amount of distance traveled in miles per hour (mile)
$PD_{t,s}^{initial}$	Initial electrical load before demand response (kW)
$Prob_s$	Probability of each scenario
$SOC_{ess/hss,t0}$	Initial SOC of ESS/HSS (kWh)
$SUC_{dg/chp}, SDC_{dg/chp}$	Startup/shutdown DG/CHP cost ($/h)

$UT_{dg}^{on}/DT_{dg}^{off}$ Minimum up/down time of each DG (h)

$pr^{PBDR/IBDR}$ Participation rate of costumers in the PBDR/IBDR programs

η^{CC} Efficiency of carbon capture process

$\mu^{CO_2,power/NG/Heat}$ Coefficient of CO2 produced when buying from the markets (kg/kWh)

$\mu_{dg/chp/boiler}^{CO_2}$ CO2 emission intensity of DG/CHP/Boiler (kg/kWh)

$\mu_{p2g}^{CO_2}$ CO2 required by P2G as input (kg/kWh)

$\pi^{IBDR,base}$ Price of load curtailment in first block ($/kW)

$\pi_{t,b}^{IBDR}$ Price of load curtailment ($/kW)

π_t^{PBDR} Pricing of consumer consumption by PBDR programs ($/kW)

$\pi_t^{power/NG/Heat}$ The day ahead electricity ($/kW)/Natural gas ($/MBTU)/Heat ($/kW) market price

π_t^{res} The spinning reserve market price ($/kW)

$\pi_t^{retail,NG/Heat}$ Retail rate of natural gas ($/MBTU)/heat ($/kW)

ρ^{CC} Carbon capture process coefficient

$[H_{chp}^{A,B,C,D}, P_{chp}^{A,B,C,D}]$ CHP operation range [kW, kW]

M Big positive number

$RU/RD_{dg,chp}$ Ramp up/down rate limit of each DG/CHP (kW/h)

a, b Unit cost coefficients ($/kWh), ($/h)

$\eta_{dg}, \eta_{P2G}, \eta_{boiler}$ DG/P2G/Boiler efficiency

Binary variables

u_t Binary variable, 1 means the unit is on and 0 means the unit is off.

Free variables

$\Delta L_{t,s}^{PBDR}$ Changes in electrical load consumption in the PBDR program (kW)

$C_{EV,t,s}$ EV charging/discharging cost ($)

$P_{t,s}^{DA}, G_{t,s}^{DA}, H_{t,s}^{DA}$ Energy exchanged with the day ahead electricity (kW)/Natural gas (MBTU)/Heat (kW) market

Integer variables

$X_{dg,t}^{on/off}$ The number of hours DG has been on/off in a row (h)

Positive variables

$\{\cdot\}^{buy}, \{\cdot\}^{sell}$ Buy/sell from/to energy markets

$\{\cdot\}^{ch}, \{\cdot\}^{dch}$ The amount of charge/discharge of the units

$\Delta L_{t,s}^{IBDR}$ The difference between the present and previous blocks' curtailed electrical load (kW)

$C_{dg,t,s}^{prod}$ Dg's production costs ($)

$C_{dg/chp,t}^{SU/SD}$ Dg/CHP startup/shutdown cost ($)

$C_{dg/chp/boiler,t,s}$ Dg/CHP/Boiler total costs ($)

$C_{ess/hss,t,s}$ Degradation cost of ESS/HSS ($)

$C_{t,s}^{IBDR}$ Cost of PBDR/IBDR programs ($)

$E_{P2G,t,s}$ The amount of pollution absorbed by P2G (kg)

$E_{t,s}^{Grid}$ The amount of pollution produced by grid (kg)

$E_{t,s}^{Total}$ The amount of pollution absorbed by carbon capture process (kg)

$E_{t,s}^{Units}$ Total pollution produced by virtual power plant units (kg)

$E_{t,s}^{power/NG/Heat}$ Pollution caused when purchasing electricity/Natural Gas/Heat from the market (kg)

$F_{dg/chp/boiler,t,s}$ Fuel consumption of each DG/CHP/Boiler (MBTU)

$G_{P2G,t,s}^{CH_4}$ The amount of natural gas produced by the P2G that is injected directly into the gas network (MBTU)

$G_{P2G,t,s}$ Output natural gas of P2G (MBTU)

$GS_{P2G,t,s}$ State of P2G gas storage (MBTU)

$H_{chp/boiler/hss,t,s}$ Thermal output of CHP/Boiler/HSS (kW)

$L_{t,b,s}^{IBDR}$ The amount of curtailed electrical load in the IBDR program (kW)

$P_{P2G,t,s}$ Input power of P2G (kW)

$P_{dg,t,s}$ Output power of DG (kW)

$P_{t,s}^{CC}$ The amount of power consumed for the carbon capture process ($)

$P_{t,s}^{res}$ Total capacity of the VPP to participate in the spinning reserve market (kW)

$Res_{dg/chp,t,s}$ Amount of DG/CHP participation in spinning reserve market (kW)

$Res_{t,s}^{IBDR}$ Amount of IBDR participation in spinning reserve market (kW)

$R_{t,s}^{power,res}$ Profits from the spinning reserve electricity market ($)

$R_{t,s}^{power/NG/Heat,DA}$ Profits from the day ahead electricity/Natural Gas/Heat market ($)

$R_{t,s}^{retail,power/NG/Heat}$ Profit of VPP from selling electrical/natural gas/thermal energy to consumers ($)

$SOC_{ess/EV/hss,t,s}$ State of charge of ESS/EV/HSS (kWh)

REFERENCES

1. Mokhtari, M., Gharehpetian, G.B., Mousavi Agah, S.M.: Distributed energy resources. In: Distributed Generation Systems: Design, Operation and Grid Integration. Ch. 1. Elsevier Inc., Amsterdam (2017)
2. Nosratabadi, S.M., Hooshmand, R.A., Gholipour, E.: A comprehensive review on microgrid and virtual power plant concepts employed for distributed energy resources scheduling in power systems. Renewable Sustainable Energy Rev. 67, 341–363 (2017)

3. Tan, Z., Fan, W., Li, H., et al.: Dispatching optimization model of gas-electricity virtual power plant considering uncertainty based on robust stochastic optimization theory. J. Cleaner Prod. 247, 119106 (2020)
4. Rahimi, M., Ardakani, F.J., Ardakani, A.J.: Optimal stochastic scheduling of electrical and thermal renewable and non-renewable resources in virtual power plant. Int. J. Electr. Power Energy Syst. 127, 106658 (2021)
5. Lorestani, A., Ardehali, M.M.: Optimization of autonomous combined heat and power system including PVT, WT, storages, and electric heat utilizing novel evolutionary particle swarm optimization algorithm. Renewable Energy 119, 490–503 (2018)
6. Van Helden, W.G.J., Van Zolingen, R.J.C., Zondag, H.A.: PV Thermal systems: PV panels supplying renewable electricity and heat. Prog. Photovoltaics Res. Appl. 12(6), 415–426 (2004)
7. Cui, H., Li, F., Hu, Q., Bai, L., Fang, X.: Day-ahead coordinated operation of utility-scale electricity and natural gas networks considering demand response based virtual power plants. Appl. Energy 176, 183–195 (2016)
8. Vahedipour-Dahraie, M., Rashidizadeh-Kermani, H., Shafie-Khah, M., Catalão, J.P.S.: Risk-Averse Optimal Energy and Reserve Scheduling for Virtual Power Plants Incorporating Demand Response programs. IEEE Trans. Smart Grid 12(2), 1405–1415 (2021)
9. Mousavi, M., Rayati, M., Ranjbar, A.M.: Optimal operation of a virtual power plant in frequency constrained electricity market. IET Gener. Transm. Distrib. 13(11), 2123–2133 (2019)
10. Arslan, O., Karasan, O.E.: Cost and emission impacts of virtual power plant formation in plug-in hybrid electric vehicle penetrated networks. Energy 60, 116–124 (2013)
11. Long, D., Moore, G., Wenban-Smith, G., Pethybridge, E., Gas, B.: Gas Trading Manual (2003)
12. Werner, S.: ECOHEATCOOL. (2005)
13. Akbari-Dibavar, A., Farahmand-Zahed, A., Mohammadi-Ivatloo, B.: Concept and glossary of demand response programs. In: Demand Response Application in Smart Grids: Concepts and Planning Issues - Volume 1. pp. 1–20. Springer, Cham (2020)
14. Nojavan, S., Zare, K., Mohammadi-Ivatloo, B.: Optimal stochastic energy management of retailer based on selling price determination under smart grid environment in the presence of demand response program. Appl. Energy 187, 449–464 (2017)
15. Majidi, M., Mohammadi-Ivatloo, B., Anvari-Moghaddam, A.: Optimal robust operation of combined heat and power systems with demand response programs. Appl. Therm. Eng. 149, 1359–1369 (2019)
16. Ju, L., Tan, Z., Yuan, J., Tan, Q., Li, H., Dong, F.: A bi-level stochastic scheduling optimization model for a virtual power plant connected to a wind-photovoltaic-energy storage system considering the uncertainty and demand response. Appl. Energy 171, 184–199 (2016)
17. Shayeghi, H., Shahryari, E., Pashaei-Didani, H., Nojavan, S.: Modeling an improved demand response program in day-ahead and intra-day markets. In: Demand Response Application in Smart Grids: Concepts and Planning Issues - Volume 1. pp. 93–111. Springer, Cham (2020)
18. Wang, Z., Paranjape, R., Chen, Z., Zeng, K.: Layered stochastic approach for residential demand response based on real-time pricing and incentive mechanism. IET Gener. Transm. Distrib. 14(3), 423–431 (2020)
19. Ghahramani, M., Sadat-Mohammadi, M., Nazari-Heris, M., Asadi, S., Mohammadi-Ivatloo, B.: Introduction and literature review of the operation of multi-carrier energy networks. In: Power Systems. pp. 39–57. Springer, Cham (2021)
20. Bostan, A., Nazar, M.S., Shafie-khah, M., Catalão, J.P.S.: Optimal scheduling of distribution systems considering multiple downward energy hubs and demand response programs. Energy 190, 116349 (2020)
21. Yang, Y., Tang, L., Wang, Y., Sun, W.: Integrated operation optimization for CCHP micro-grid connected with power-to-gas facility considering risk management and cost allocation. Int. J. Electr. Power Energy Syst. 123, 106319 (2020)
22. Zare Oskouei, M., Nahani, H., Mohammadi-Ivatloo, B., Abapour, M.: Optimal scheduling of hybrid energy storage technologies in the multi-carrier energy networks. In: Power Systems. pp. 143–157. Springer, Cham (2021)
23. Mirzaei, M.A., Oskouei, M.Z., Mohammadi-Ivatloo, B., et al.: Integrated energy hub system based on power-to-gas and compressed air energy storage technologies in the presence of multiple shiftable loads. IET Gener. Transm. Distrib. 14(13), 2510–2519 (2020)
24. Hadayeghparast, S., SoltaniNejad Farsangi, A., Shayanfar, H.: Day-ahead stochastic multi-objective economic/emission operational scheduling of a large scale virtual power plant. Energy 172, 630–646 (2019)
25. Ju, L., Zhao, R., Tan, Q., Lu, Y., Tan, Q., Wang, W.: A multi-objective robust scheduling model and solution algorithm for a novel virtual power plant connected with power-to-gas and gas storage tank considering uncertainty and demand response. Appl. Energy 250, 1336–1355 (2019)
26. Moghaddam, A.A., Seifi, A., Niknam, T., Alizadeh Pahlavani, M.R.: Multi-objective operation management of a renewable MG (micro-grid) with back-up micro-turbine/fuel cell/battery hybrid power source. Energy 36(11), 6490–6507 (2011)
27. Lekvan, A.A., Habibifar, R., Moradi, M., Khoshjahan, M., Nojavan, S., Jermsittiparsert, K.: Robust optimization of renewable-based multi-energy micro-grid integrated with flexible energy conversion and storage devices. Sustainable Cities Soc. 64, 102532 (2021)
28. Shahkoomahalli, A., Koochaki, A., Shayanfar, H.: Risk-based electrical-thermal scheduling of a large-scale virtual power plant using downside risk constraints for participating in energy and reserve markets. Arab. J. Sci. Eng. 47, 2663–2683 (2021)
29. Gougheri, S.S., Jahangir, H., Golkar, M.A., Ahmadian, A., Aliakbar Golkar, M.: Optimal participation of a virtual power plant in electricity market considering renewable energy: A deep learning-based approach. Sustainable Energy Grids Networks 26, 100448 (2021)
30. Zamani, A.G., Zakariazadeh, A., Jadid, S.: Day-ahead resource scheduling of a renewable energy based virtual power plant. Appl. Energy 169, 324–340 (2016)
31. Naghdalian, S., Amraee, T., Kamali, S., Capitanescu, F.: Stochastic Network-Constrained Unit Commitment to Determine Flexible Ramp Reserve for Handling Wind Power and Demand Uncertainties. IEEE Trans. Ind. Inf. 16(7), 4580–4591 (2020)
32. Heydari, R., Nikoukar, J., Gandomkar, M.: Optimal operation of virtual power plant with considering the demand response and electric vehicles. J. Electr. Eng. Technol. 16(5), 2407–2419 (2021)
33. Nourollahi, R., Zare, K., Nojavan, S.: Energy management of hybrid AC-DC microgrid under demand response programs: Real-time pricing versus timeof- use pricing. In: Demand Response Application in Smart Grids: Operation Issues - Volume 2. pp. 75–93. Springer, Cham (2019)
34. Rabiee, A., Sadeghi, M., Aghaeic, J., Heidari, A.: Optimal operation of microgrids through simultaneous scheduling of electrical vehicles and responsive loads considering wind and PV units uncertainties. Renewable Sustainable Energy Rev. 57, 721–739 (2016)
35. U.S. Department of Transportation, Federal Highway Administration, 2017 National Household Travel Survey. http://nhts.ornl.gov. Accessed 15 January 2022
36. Xu, Y., Dong, Z.Y., Zhang, R., Hill, D.J.: Multi-timescale coordinated voltage/var control of high renewable-penetrated distribution systems. IEEE Trans. Power Syst. 32(6), 4398–4408 (2017)
37. Mavrotas, G.: Effective implementation of the ε-constraint method in multi-objective mathematical programming problems. Appl. Math. Comput. 213(2), 455–465 (2009)
38. Soroudi, A.: Simple examples in GAMS. In: Power System Optimization Modeling in GAMS. pp. 33–63. Springer, Cham (2017)
39. Ahmadi, A., Mavalizadeh, H., Zobaa, A.F., Ali Shayanfar, H.: Reliability-based model for generation and transmission expansion planning. IET Gener. Transm. Distrib. 11(2), 504 (2017)
40. Soroudi, A.: Dynamic economic dispatch. In: Power System Optimization Modeling in GAMS. pp. 95–118. Springer, Cham (2017)
41. Hosseinnia, H., Nazarpour, D., Talavat, V.: Utilising reliability-constrained optimisation approach to model microgrid operator and private investor participation in a planning horizon. IET Gener. Transm. Distrib. 12(21), 5798–5810 (2018)
42. Home | Ontario Energy Board. https://www.oeb.ca/ Accessed 15 August 2021

43. EIA: U.S. Price of Natural Gas Delivered to Residential Consumers (Dollars per Thousand Cubic Feet). https://www.eia.gov/dnav/ng/hist/n3010us3A.htm Accessed 15 August 2021
44. Alipour, M., Mohammadi-Ivatloo, B., Zare, K.: Stochastic scheduling of renewable and CHP-based microgrids. IEEE Trans. Ind. Inf. 11(5), 1049–1058 (2015)
45. Carbon dioxide emissions by fuel: Environment - U.S. Energy Information Administration (EIA) - U.S. Energy Information Administration (EIA). https://www.eia.gov/environment/emissions/co2_vol_mass.php Accessed 15 August 2021

How to cite this article: Ghasemi Olanlari, F., Amraee, T., Moradi-Sepahvand, M., Ahmadian, A.: Coordinated multi-objective scheduling of a multi-energy virtual power plant considering storages and demand response. IET Gener. Transm. Distrib. 16, 3539–3562 (2022). https://doi.org/10.1049/gtd2.12543